

RU 153

153
DE

3854

ANNUAL REPORT

CIRCULATION PROCESSES IN
BRISTOL BAY, ALASKA USING DISSOLVED
METHANE AS A TRACER

Prepared by

Joel Cline, Charles Katz, and Herbert Curl, Jr.

Pacific Marine Environmental Laboratory

7600 Sand Point Way N.E.

Seattle, Washington 98115

TABLE OF CONTENTS

	<u>Page</u>
Figures	iii
1. GENERAL SUMMARY	1
1.1 Objectives of Program	1
1.2 Summary of Preliminary Observations	1
2. INTRODUCTION	3
2.1 Purpose of Study	3
2.2 Objectives	3
2.3 Relevance to OCSEAP	4
3. STUDY AREAS	5
3.1 Bristol Bay	5
3.2 North Aleutian Shelf	7
3.3 St. George Basin	8
4. METHODOLOGY	9
4.1 Sample Collection	9
4.2 Preconcentration	9
4.3 Gas Chromatography	10
5. RESULTS.	10
5.1 North Aleutian Shelf	10
5.2 St. George Basin	22
6. DISCUSSION	30
6.1 Plume Model	30
6.1.1 Model Scenarios	34
6.1.2 Model Fit	37
6.2 St. George Basin	41
6.2.1 Vertical Methane Distribution	42
6.2.2 Near-Bottom Methane Plume	48
References	52

FIGURES

<u>Number</u>		<u>Page</u>
1	Regional setting of southeastern Bering Sea including Bristol Bay.	6
2	NAS stations occupied in August, 1980.	11
3	Surface salinity (g/kg) distribution along the NAS in August, 1980.	12
4	Surface concentration of dissolved methane (nL/L) along the NAS in August, 1980.	13
5	Vertical profiles of dissolved methane along two sections normal to the NAS. Sections IV and V are immediately east of Port Moller.	15
6	Distribution of methane across the entrance of Port Moller during a 24-hour tidal cycle. The vertical bars indicate 1σ variation in the mean concentration at each station. The largest variation was observed at station PM-3, near the eastern side of Port Moller.	16
7	NAS stations occupied in February, 1981.	17
8	Surface salinity distribution (g/kg) along the NAS in February, 1981.	18
9	Surface distribution of dissolved methane (nL/L) along the NAS in February, 1981.	20
10	Correlations between temperature ($^{\circ}$ C), salinity (g/kg), methane (nL/L) and tidal amplitude (m) at station PM-3 in February, 1981.	21'
11	St. George Basin stations occupied in August, 1980.	23
12	Vertical distribution of salinity (a), σ_t (b), methane (c) and temperature (d) along the PROBES Line in August, 1980. The middle front is located near PL8-10.	24
13	Near-bottom distribution (B-5 m) of methane (nL/L) in St. George Basin in August, 1980. Maximum concentrations were found near stations PI-6 and SG-5.	25
14	St. George Basin stations occupied in February, 1981.	27
15	Vertical distribution of methane along a portion of the PROBES Line in February, 1981.	28
16	Near-bottom distribution (B-5 m) of methane (nL/L) in St. George Basin in February, 1981. Maximum concentration was observed at station SG-28; which is south of PL-6.	29

FIGURES

<u>Number</u>		Page
17	Model schematic of the NAS. The significant transport terms are horizontal diffusion, $K_x C''$, and horizontal advection, $V_x C'$. The well mixed coastal water is 10 km wide and 15 m deep.	35
18	Relative concentrations of methane, depth integrated, predicted from equation (2), assuming various mean velocities of (a) 5 cm s, (b) 7.5 cm s and (c) 10 cm s. Air-sea exchange of methane and biological oxidation are included in a single first order rate constant, $k = 4.6 \times 10^{-7}$ s. Source strength is set at 8-10 km.	36
19	A comparison of a observed methane distribution (solid lines) with the 7.5 cm s model scenario. Pulsing of the estuary leads to a strong time dependent source, which is not accommodated by the stationary model.	38
20	Tidal range and maximum ebb and flood tidal velocities at Entrance Point, Port Moller. The data presumably reflect conditions at mid-channel. Data are from the NOAA tide tables covering the observational period.	39
21	Vertical density distribution at PL-6 on August 29, 1980 and September 3, 1980. Note the effects of salt fingering and double-diffusion.	43
22	Vertical distribution of dissolved methane at PL-6 on August 29, 1980 and September 3 1980	44
23	Estimated apparent vertical eddy diffusivity or a function of the buoyancy gradient. The Brunt-Vaaisela frequency was determined from the density distribution; K_v from the observed methane profile. The reciprocal square-root relationship suggests shear-induced turbulence.	46
24	A model fit to the depth integrated methane profile in the lower boundary layer ($\Delta z \sim 30$ m). The two case studies are (a) $\bar{u} = 2.5$ cm s^{-1} and (b) $\bar{u} = 5.0$ cm S-l. The length of the source was assumed to be 30 km. The biological oxidation rate constant for the destruction of methane was set equal to 3.0×10^{-8} S-l.	50

1. GENERAL SUMMARY

1.1 Objectives of Program

The goal of this study is to utilize dissolved methane as a Lagrangian tracer of petroleum introduced from point sources in Bristol Bay, Alaska. Previous baseline studies in this area revealed the presence of localized sources of methane in Port Moller, an estuary along the North Aleutian Shelf (NAS), and in the bottom waters of St. George Basin (SGB). Both the NAS and SGB are potential gas and oil lease areas and thus may eventually be subjected to a point source introduction of petroleum. In order to determine the fate and impact of spilled oil, it is of paramount importance to elucidate mean flow trajectories, velocities and turbulence regime.

1.2 Summary of Preliminary Observations

Two cruises have been conducted in Bristol Bay to date for this program. The first, in August, 1980, emphasized the NAS region. More time was dedicated to SGB in February, 1981, although the major effort was still on the NAS. On both occasions measurements of methane, suspended matter, mass field, currents (utilizing current meters) and microbiological methane production and consumption rates were made. Only observations from August are considered here in depth.

The major feature of the methane distribution on the NAS is the methane plume emanating from Port Moller in a well defined trajectory to the east. The plume could be traced to Port Heiden, approximately 150 km down the coast. Dissolved methane remains in the coastal zone and rarely penetrates more than 20 km

offshore. Assuming a stationary condition, the average mean velocity along the coast as calculated from a diffusion-advection model would be $7 \text{ cm s}^{-1} \pm 2 \text{ cm s}^{-1}$. Port Moller does not represent a uniform source of methane, but rather appears to pulse every 28 days, in concert with the occurrence of perigean tides. The aforementioned model allows for a scaled diffusion coefficient and predicts cross-shelf values ranging from $10^5 \text{ cm}^2 \text{ s}^{-1}$ to $10^6 \text{ cm}^2 \text{ s}^{-1}$. These values are systematically smaller than those computed for salt and is an artifact of the scale of the methane plume. However, when considering point source introductions of petroleum, dissolved methane is a useful tracer of these length scales.

The plume of methane observed in the near-bottom waters of St. George Basin was elongated in the northwest-southeast direction, apparently bathymetrically contained. Dissolved methane was uniformly distributed in the lower 30 m of the water column in agreement with other water column properties. Assuming a one-dimensional flux model with the surface flux as a boundary condition, apparent vertical eddy diffusivities (K_v) were calculated across the pycnocline. A plot of the apparent diffusivities versus the Brunt-Vaisela frequency gave a $-1/2$ power relationship suggesting shear induced turbulence. Two dynamic mixing regimes were apparent, the first in the upper portion of the pycnocline was characterized with K_v 's ranging $20\text{-}50 \text{ cm}^2 \text{ s}^{-1}$. The lower region was much less turbulent, with volumes ranging $0.2\text{-}0.5 \text{ cm}^2 \text{ s}^{-1}$. During periods of stratification, the lower boundary layer is well insulated from vertical exchange. Preliminary modeling efforts suggest a mean flow in the lower boundary layer of approximately 5 cm s^{-1} toward the northwest, in excellent agreement with current meter measurements. The penetration of the plume to the southeast, nearly to Unimak Pass, suggests periodic weakening or reversal of the mean northwest flow. It is apparent that along-shelf dispersion is more active than cross-shelf, which is in agreement with the distribution of mass.

2. INTRODUCTION

2.1 Purpose of Study

The purpose of this program is to use naturally-occurring sources of dissolved methane as a Lagrangian tracer of mean circulation in selected subregions of Bristol Bay, Alaska. Regardless of the origin of the methane, point sources allow estimates to be made of trajectories, mean velocities and horizontal dispersion coefficients. Because of the nature of the methane sources, the behavior of other dissolved materials introduced from point sources (e.g., surface spills, well blowouts, etc.) can be elucidated. By analyzing the plume distribution of methane, correcting for biological consumption and air-sea exchange and introducing mean current velocities derived from current meter measurements, estimates can be made of the scale of turbulence.

2.2 Objectives

The principal goal of this study is to use dissolved methane as a quantitative tracer of circulation processes and mixing dynamics in selected areas of Bristol Bay, Alaska, a large embayment located in the southeastern Bering Sea. This report deals with two site specific areas of Bristol Bay, the NAS and SBG. Specifically, the objectives are:

1. To quantify the longshore mean velocity and cross-shelf dispersion coefficients along the NAS using a point source of methane emanating from the Port Moller estuary.
2. To estimate near-bottom current trajectories and lateral dispersion coefficients in St. George Basin, using a bottom source of methane as a tracer.

3. To estimate the depth dependent vertical eddy diffusivity in St. George Basin using a one-dimensional vertical flux, model.
4. To analyze the distributions of methane in terms of a two-dimensional diffusion-advection model for the purpose of confirming mean current velocities and estimating the magnitude of horizontal and vertical processes.

2.3 Relevance to OCSEAP

The persistence of oil in Bristol Bay depends on several physical, chemical and biological processes that act in concert to disperse and degrade petroleum. These processes, each with their characteristic time scale (i.e., half-life), must be considered together in order to determine a characteristic time (or space) scale for the persistence of oil. Circulation and mixing processes are characterized by relatively short time scales and thus represent a first-order process. Given that the volume of spilled oil is small compared to the volume of water in the region, it is anticipated that harmful impacts due to petroleum development will be limited to space scales less than 100 km.

Utilization of methane as a diagnostic tracer of circulation and dispersion in support of the physical oceanography program, allows mesoscale mixing processes to be more clearly defined. In particular, these studies allow quantitative predictions of water mass trajectories, dispersion characteristics and water mass residence times required in order to quantitate the impact of oil on living resources.

3. STUDY AREAS

3.1 Bristol Bay

Bristol Bay is a shallow embayment located in the southeastern portion of the Bering Sea. The area and volume of the region, computed out to the 200 m isobath, is 419,000 km² and 30,000 km³, respectively, given a mean depth of approximately 70 m. Freshwater input occurs primarily from the Kuskokwim and Kvichak Rivers, located on the northern and eastern sides of the bay (Fig. 1), resulting in a 2‰ salinity difference between the offshore waters and the near-shore areas (Schumacher et al., 1979).

Bristol Bay is characterized by a series of frontal features, primarily located at distinct bathymetric depths (Kinder and Schumacher, 1981). These fronts occur roughly at the 200 m (shelf break front), 100 m (middle shelf) and 50 m (inner front) isobaths (see Fig. 4-1; Kinder and Schumacher, 1981a). Mean circulation landward of the middle front is presumed weak (≤ 2 cm S-1) and hydrographic structures are largely determined by buoyancy input, wind stirring and tidal mixing (Kinder and Schumacher, 1981a, see their report for details). There appears to be a weak cyclonic circulation around the perimeter of Bristol Bay, largely confined to the coastal zone ($Z \leq 50$ m).

Bristol Bay is partially ice covered in winter, usually beginning in protected bays in November and builds to a maximum in March. The spring melting results in considerable freshwater added to the surface (Schumacher et al., 1979). Maximum ice coverage is approximately 60%; thickness is usually less than 1 m. Details on hydrography and climate of the region can be found in reports by Kinder and Schumacher, 1981a; Kinder and Schumacher, 1981b; Coachman and Charnell, 1979; Overland, 1981; and references contained therein.

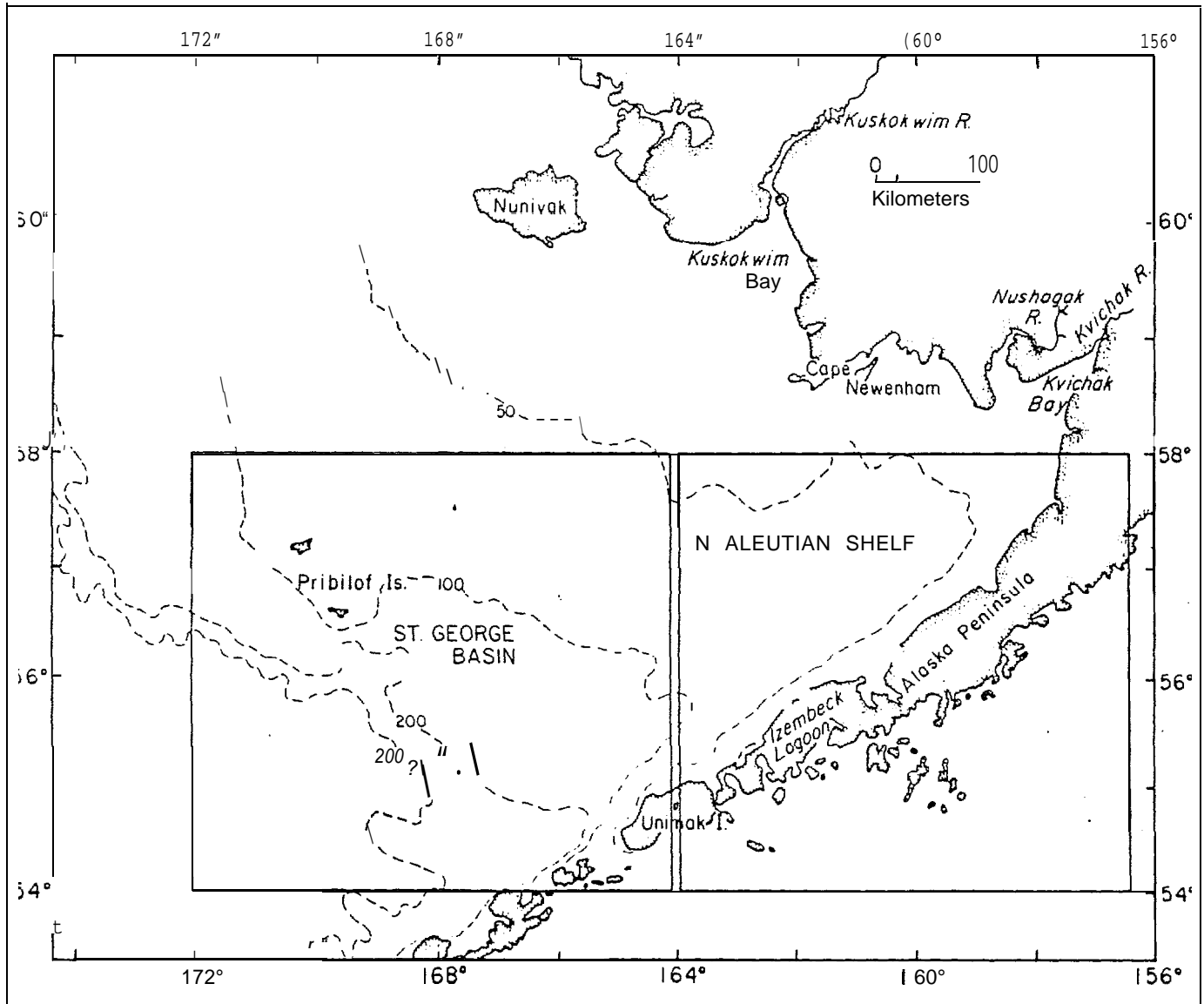


Figure 1. Regional setting of southeastern Bering Sea including Bristol Bay.

3.2 North Aleutian Shelf (NAS)

The NAS region encompasses the near shore areas from Unimak Island on the west to the Kvichak River on the east (Fig. 1). This region is characterized by a vertically well mixed coastal zone ($Z \leq 50$ m), which is hydrographically separated from the stratified regime located seaward. The breakdown of vertical stratification in the coastal zone is reportedly due to dissipation of tidal energy (Kinder and Schumacher, 1981a).

There is no apparent major source of freshwater along the NAS, except at the eastern extremity. There are undoubtedly numerous diffuse sources, including the possibility of submarine aquifers originating in the mountains of the Aleutian Chain. Mean velocities are estimated at no more than $3\text{-}5 \text{ cm s}^{-1}$ to the east (Schumacher et al., 1979), but there also appears to be strong seasonal variability in direction and magnitude (Personal communication, J. Schumacher).

The principal embayment along the NAS, Port Moller, is comprised of two arms, each approximately 38 km in length, with mean depths ranging from 5 m to 15 m. The western arm, Herendeen Bay, is the deeper of the two with a deep inner basin (approximately 100 m). Tidal currents within the Port Moller-Herendeen Bay complex are relatively strong, reaching maximum ebb and flood velocities of approximately 150 cm s^{-1} (Department of Commerce, 1981).

Previous measurements made in September-October of 1975 and again in July of 1976 (Cline, 1981), revealed that the Port Moller estuary represented a significant source of dissolved methane to the surface waters that could be traced down the coast (east) for distances of 200 km. The source of methane within Port Moller was not specifically known, but was believed to arise from methanogenesis in anoxic marine muds or possibly from the cannery operations

at Port Moller. Observations made in the summer of 1980 and again in winter of 1981 now shed some light on the source of methane.

3.3 St. George Basin

St. George Basin is an offshore basin located near the shelf break in Bristol Bay (Fig. 1). The axis of the basin is northwest-southeast, running roughly from Unimak Pass to the Pribilof Islands. The basin proper is largely contained between the 100-200 m isobaths.

The basin waters are separated from the inner shelf by the middle front at about 100 m and from the Bering Sea water located seaward of the 200 m isobath (Kinder and Schumacher, 1981a; see their Fig. 4-1). Dynamic topographies are largely oriented parallel to the isobaths and reflect weak mean currents toward the northwest (Coachman and Charneil, 1979). Although seasonal variations do exist, surface and near-bottom mean currents are usually $\leq 5 \text{ cm s}^{-1}$ as confirmed from moored current meters (Coachman and Charneil, 1979; Kinder and Schumacher, 1981).

The waters overlying SGB appear to be seasonally stratified. There is a strong erosion and deepening of the pycnocline in winter. Because Alaska Stream-Bering Sea water penetrates the shelf seasonally (Kinder and Schumacher, 1981), it is expected that the basin water is modified seasonally by cross-shelf advection and diffusion. Because the water column is seasonally stratified and characterized by weak mean currents, the injection of petroleum or other contaminants is of particular concern.

4. METHODOLOGY

4.1 Sample Collection

Water samples were collected using standard 5 L Niskin[®] bottles mounted on a General Oceanics Rosette sampler. Once on deck, water was transferred to clean 1 L glass-stoppered bottles such that air bubbles were not trapped. The samples were stored in the dark at approximately 5°C until analyzed, which was usually performed within one hour.

4.2 Preconcentration

The analysis of methane was accomplished using a procedure adopted from that originally proposed by Swinnerton and Linnenbom (1967). A detailed discussion of the methods used for analyzing methane and other LMW hydrocarbons can be found in Katz (1980). Dissolved methane was removed from approximately 250 mL of seawater by helium stripping. Gases removed from solution were passed through Drierite[®], Ascarite[®] and Tenax G.C.[®] traps to remove water vapor, carbon dioxide and heavier hydrocarbons. Methane was concentrated on an activated alumina trap at -196°C. After quantitative removal from solution, (~ 5 minutes at a helium flow rate of 100 mL min⁻¹) the trap was warmed to 100°C and the methane was backflushed directly into a gas chromatography.

4.3 Gas Chromatography

Detection of methane was carried out on a Hewlett-Packard 5710A gas chromatography equipped with dual flame ionization detectors. In order to insure separation of methane from the air gases (N₂ and O₂), chromatography was accomplished with an activated alumina 60-80 mesh column (1.8 m x 0.48 cm). Chromatography was completed in less than two minutes at a carrier flow rate.

of 50 mL min⁻¹ and the oven held isothermally at 100° C. Quantitation was accomplished by comparing the samples with methane standards of known concentration.

5. RESULTS

5.1 North Aluetian Shelf

The station grid occupied in August, 1980 is shown in Figure 2. Emphasis was placed on the vertical and horizontal distributions of salinity, temperature and dissolved methane. Several of the sections were occupied repeatedly during the duration of the study to provide temporal variability and model boundary conditions.

The surface salinity distribution along the NAS is shown in Figure 3. The salient features include low salinity water near the coast and the appearance of relatively high salinity water penetrating toward the east, offshore of the inner front. Just prior to sampling a major storm passed through the area (tropical storm Marge), which resulted in the temporary destruction of the inner frontal system and may have resulted in the patchy salinity distribution observed just east of Port Moller (personal communication, C. Pearson, PMEL). Port Moller appears to be the major source of freshwater between Izembek Lagoon and the Kvichak River. Port Heiden is undoubtedly a secondary source. Details on the hydrographic conditions during the observational period will be discussed by Schumacher et al. in their annual report.

The areal surface distribution of dissolved methane is shown in Figure 4. Concentrations of dissolved methane varied from near 4000 nL L⁻¹ near the entrance of Port Moller to approximately 400 nL L⁻¹ at the eastern extremity of the region (Kvichak Bay). Concentration seaward of the inner front were .

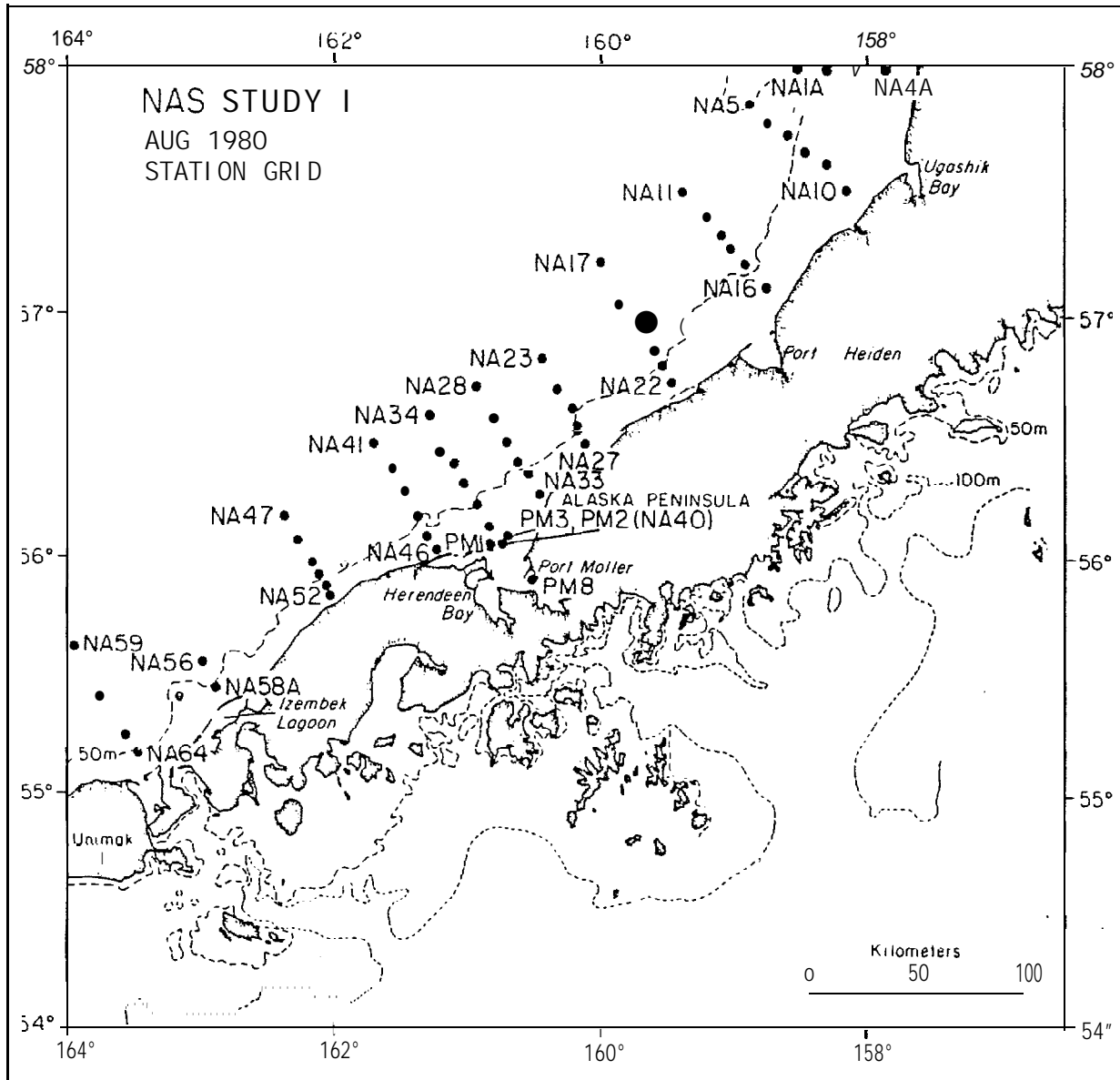


Figure 2. NAS stations occupied in August, 1980.

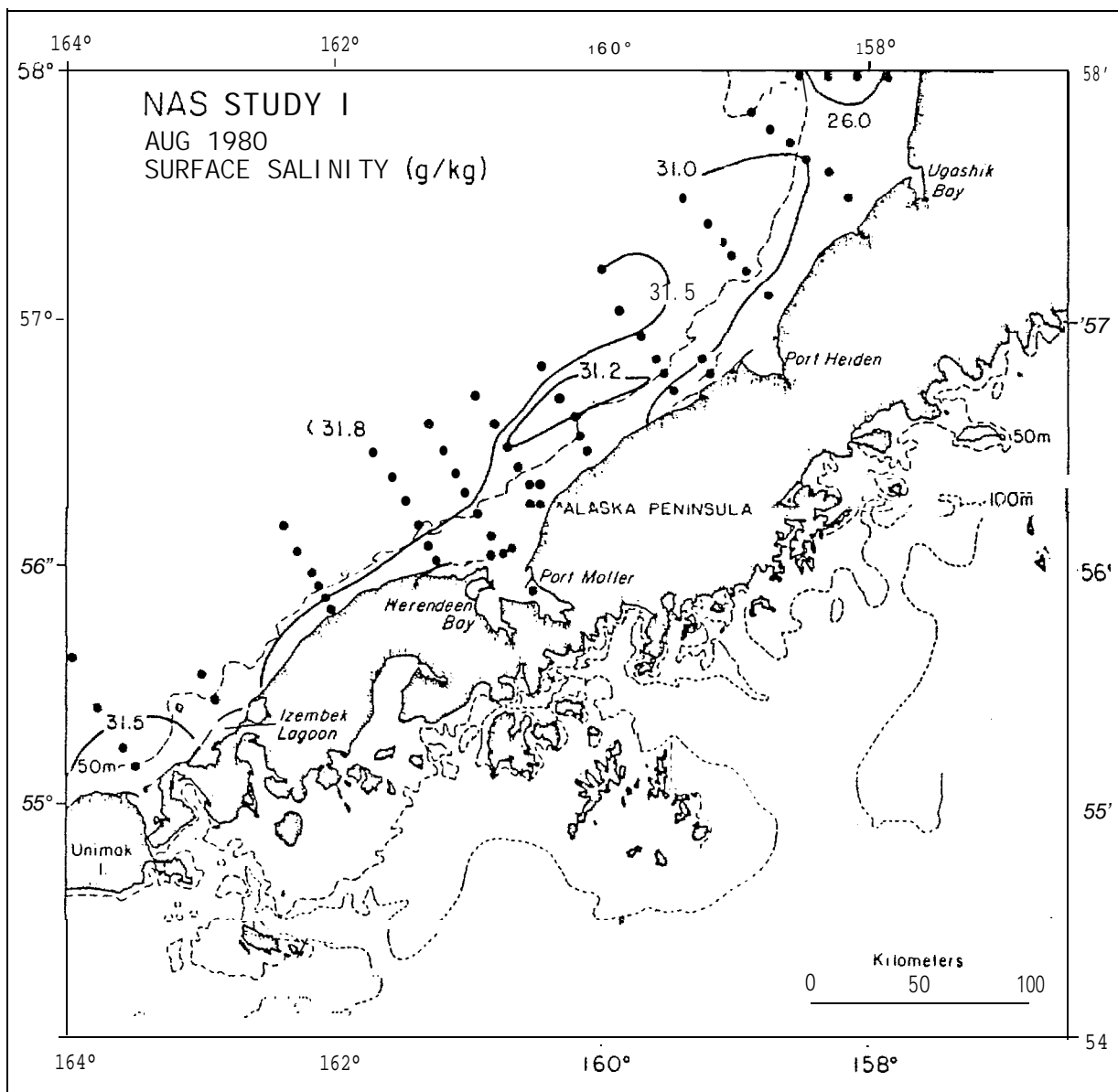


Figure 3. Surface salinity (g/kg) distribution along the NAS in August, 1980.

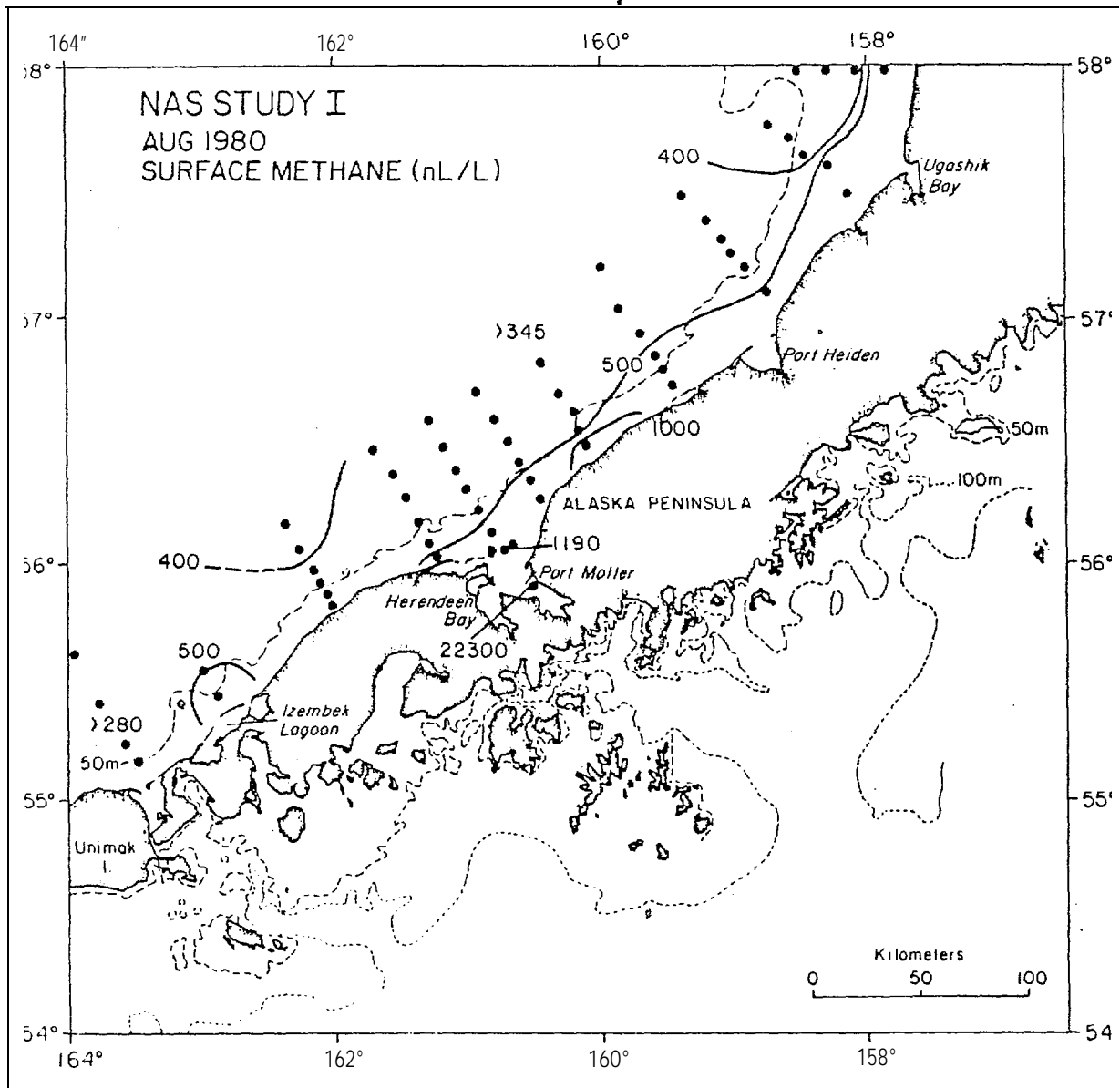


Figure 4. Surface concentration of dissolved methane (nL/L) along the NAS in August, 1980.

between 350-400 nL L⁻¹. Because the coastal zone was well mixed, the concentration of methane was vertically homogeneous, particularly near shore, as depicted in Figure 5. Surface intrusion of high methane, low salinity water is evident in several of the sections.

A minimal sampling program was conducted in the Port Moller estuary. The highest concentration of methane was found at the surface just south of the cannery located at Entrance Point. Here the concentration was near 22,000 nL L⁻¹, representing a supersaturation of 400%. Similar surface samples collected near the cannery pier were in the range of 4000-6000 nL L⁻¹, suggesting that the cannery may not be the major source of organic matter and subsequent production of methane.

In order to establish source boundary conditions for the transport of methane east along the coast, time series measurements were made across the entrance to Port Moller. A total of three stations (PM 1, 2 and 3) were occupied sequentially every two hours over a 24 hour time period. The results of this study are shown in Figure 6. Station NA-46, located on section line III just west of Port Moller, was occupied twice during the cruise. The PM stations were sampled at various stages of the tide. This diagram shows high methane water moving out alongshore to the east and being replaced by low methane water from the west. Because of shoals located near Entrance Point, it was not possible to evaluate the concentration field near shore, which is estimated by the dashed line. The shape of the curve shows strong lateral separation of the tidal flow into and out of Port Moller. The February, 1981 NAS station grid is shown in Figure 7. The surface distribution of salinity, as observed in February, 1981, is shown in Figure 8. The mean salinity field is elevated compared to conditions in August, 1980, but similar

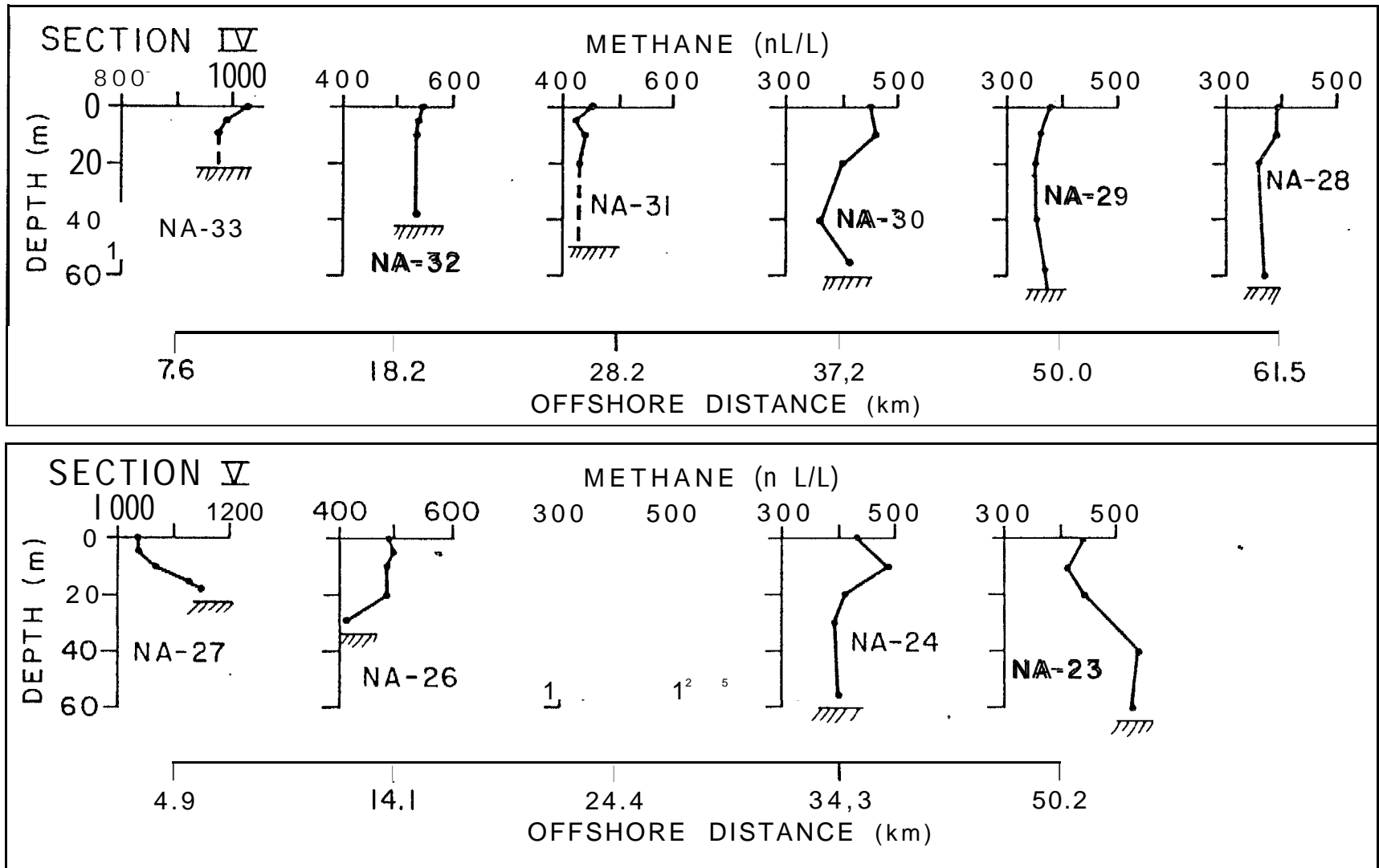


Figure 5. Vertical profiles of dissolved methane along two sections normal to the NAS. Sections IV and V are immediately east of Port Moller.

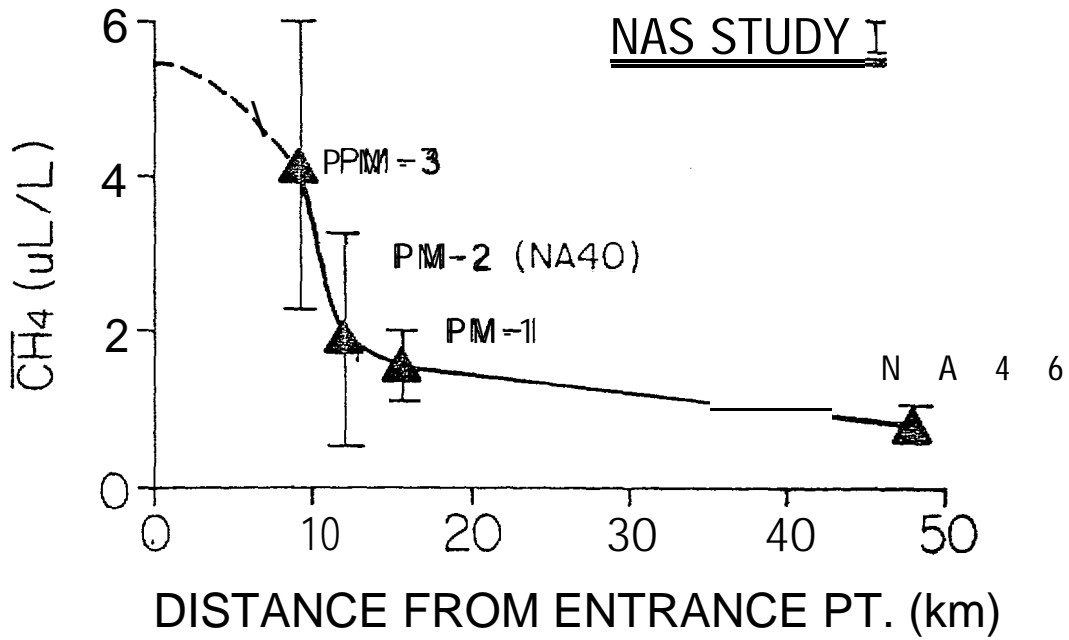


Figure 6. Distribution of methane across the entrance of Port Moller during a 24-hour tidal cycle. The vertical bars indicate 1σ variation in the mean concentration at each station. The largest variation was observed at station PM-3, near the eastern side of Port Moller.

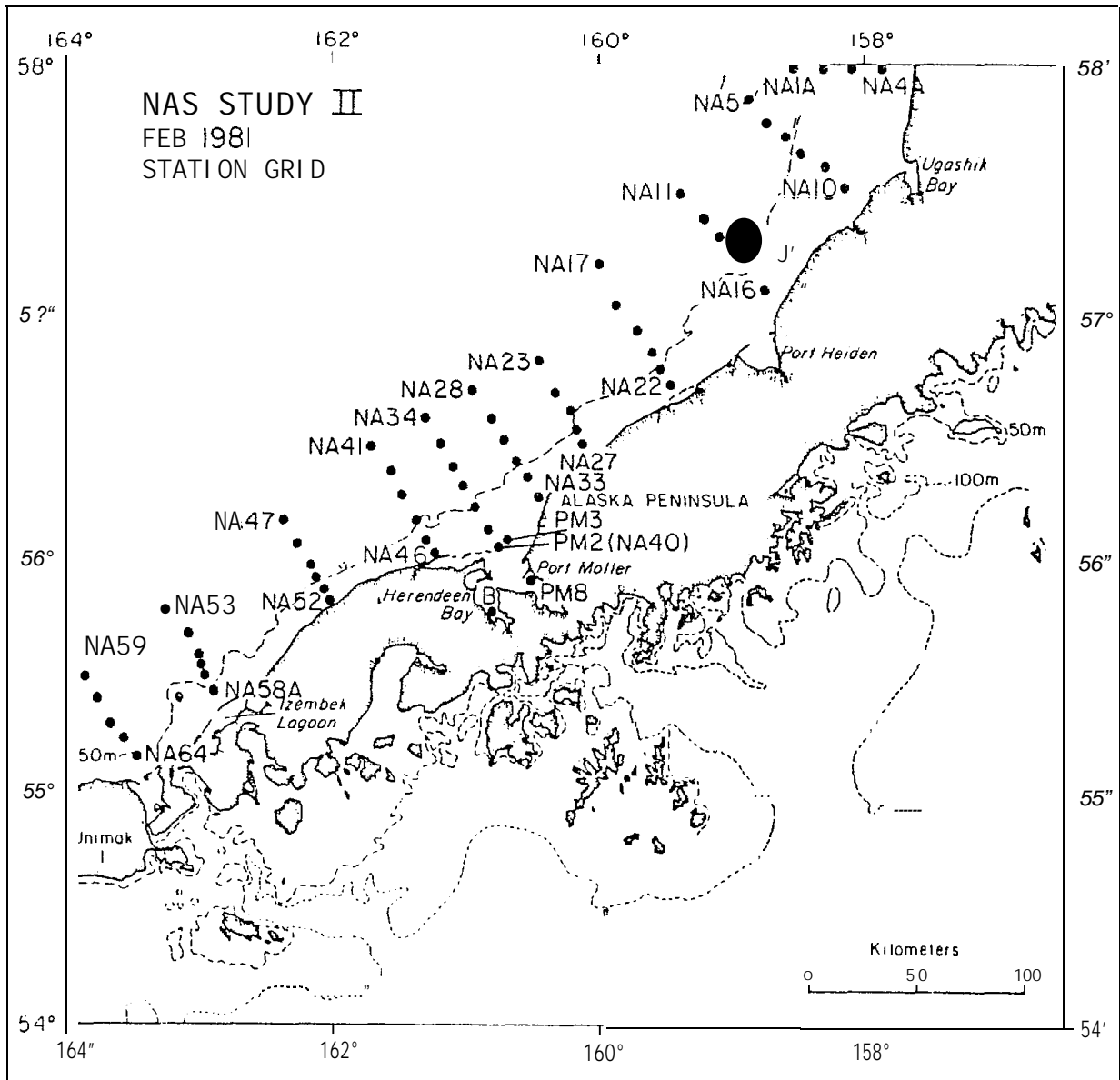


Figure 7. NAS stations occupied in February? 1981

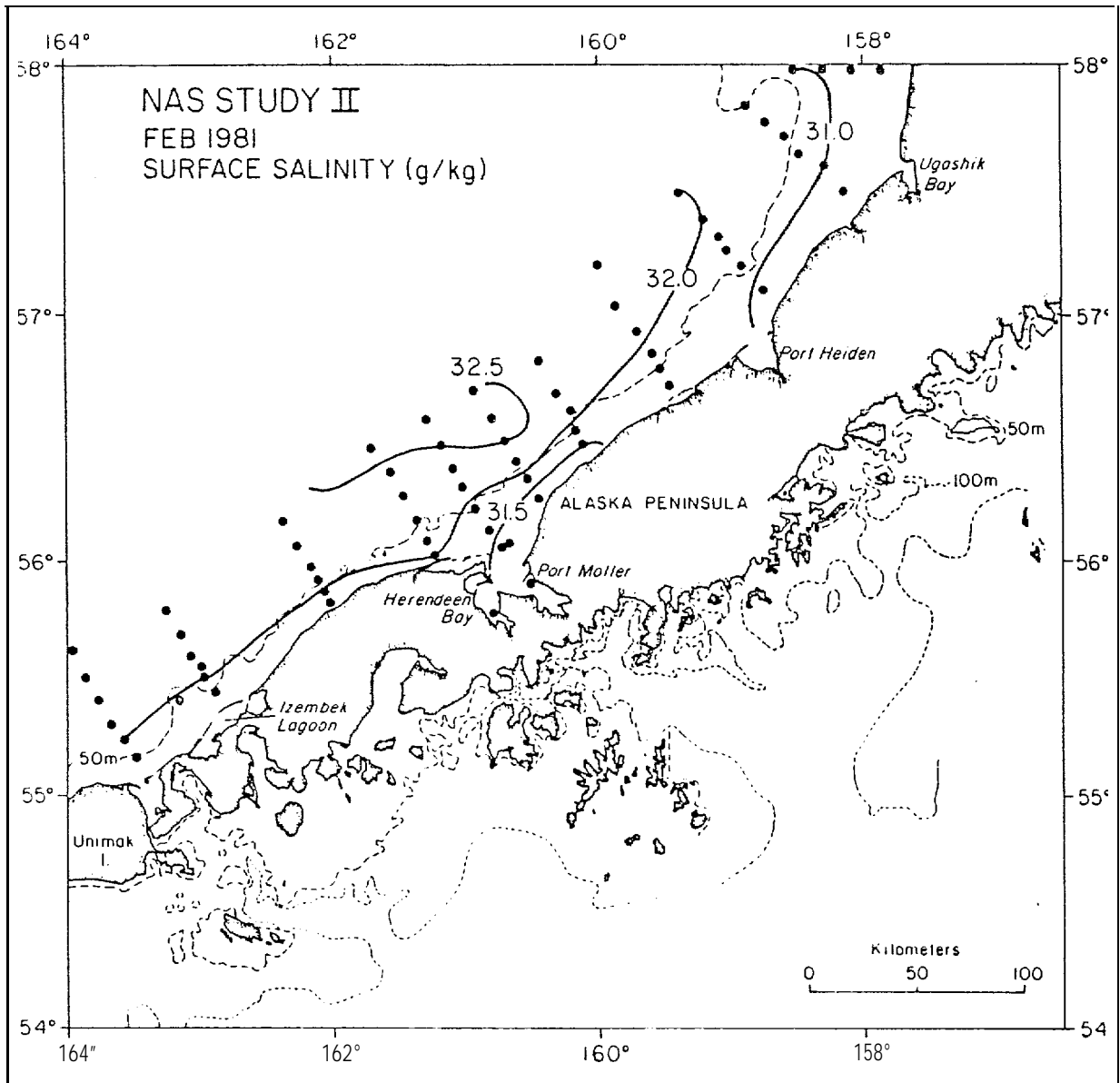


Figure 8. Surface salinity distribution (g/kg) along the NAS in February, 1981.

horizontal distributions are evident. The plume of brackish water fluxing from the Port Moller estuary is again evident, with higher salinity water found offshore.

The surface distribution of dissolved methane for the same period is shown in Figure 9. Concentrations of methane at the entrance were near 1200 nL L^{-1} , as compared to 400 nL L^{-1} observed in August, 1980. Similarly, offshore concentrations had decreased to 200 nL L^{-1} or about a factor of two relative to summer conditions. As observed previously in August, 1980, the methane flux from Port Moller was evident. The longitudinal gradient again decreased to the east. The reduced methane signature may be due to several factors-, including a reduced microbiological production rate, more vigorous stirring of the surface layer due to seasonal increases in the scalar wind speed, or a reduced flushing of the estuary because of a seasonal decrease in the freshwater supply.

The highest concentration of methane ($23,800 \text{ nL L}^{-1}$) was observed in Herendeen Bay, the western arm of Port Moller. Apparently, the anoxic muds of this small basin (100 m deep; 22 m sill⁵) provide a suitable environment for methanogenesis. Measurements of methane production rates in Herendeen Bay support this general conclusion (Griffiths, 1981). Thus, it appears that a substantial fraction of methane flux from the estuary is derived from Herendeen Bay. The previously reported high concentration of methane south of the cannery was probably due to complex tidal circulation in the estuary.

The methane flux from Port Moller is strongly correlated with low salinity water. This is graphically shown in Figure 10 for February, 1981 where correlations between salinity, methane and tidal amplitude are clearly depicted.

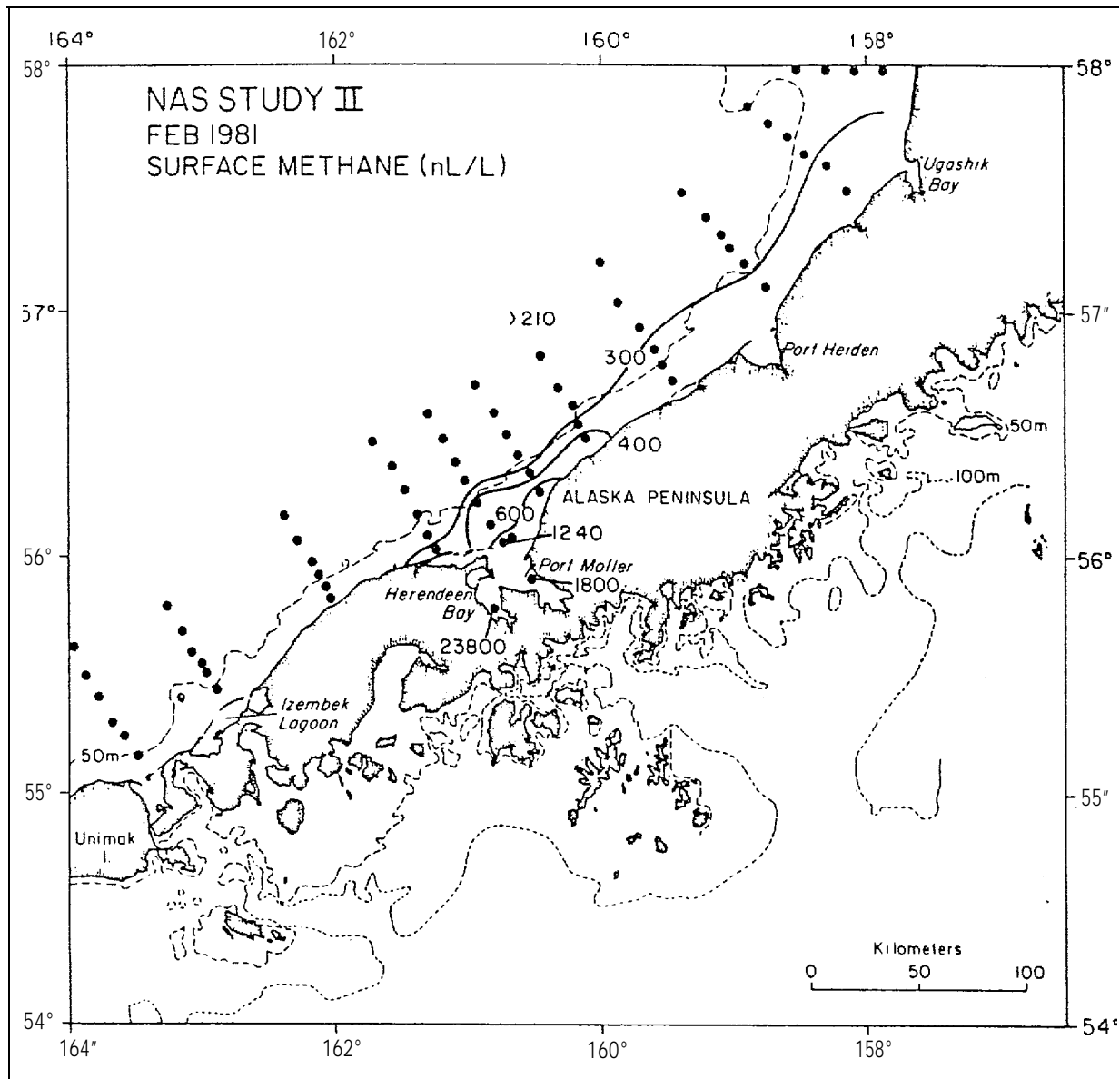


Figure 9. Surface distribution of dissolved methane (nL/L) along the NAS in February, 1981,

5-6 Feb 1981

● Surface
○ Bottom

Temperature
(°C)

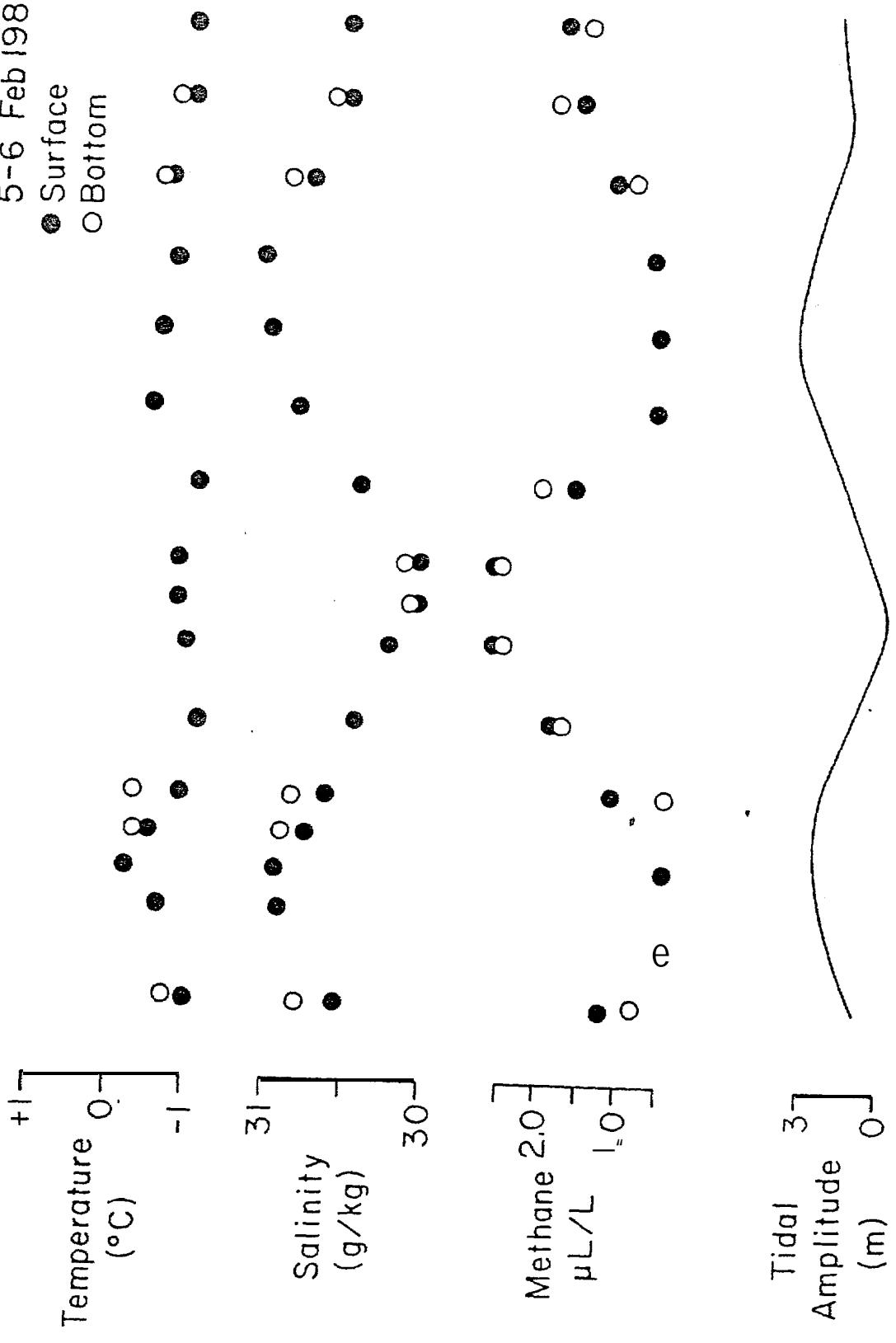
Salinity
(g/kg)

Methane
μL/L

Tidal
Amplitude
(m)

0 4 8 12 16 20 24
TIME, hours

Figure 10. Correlations between temperature (°C), salinity (g/kg), methane (nL/L) and tidal amplitude (m) at station PM-3 on February, 1981.



In the discussion section to follow, we will discuss these observations in terms of a two-dimensional steady state plume model. Only the August, 1980 data will be modeled as the data processing for the February, 1981 cruise has not progressed sufficiently to allow calculations to be made.

5.2 St. George Basin

Station locations for the August, 1980 cruise are shown in Figure 11. Detailed coverage of the area was not possible during this cruise because of the emphasis placed on the NAS. The station prefix - PL - refers to the PROBES line, which was occupied during this cruise and subsequent cruises.

The salinity distribution along the PL is shown in Figure 12a. This distribution suggests classical estuarine circulation with low salinity water at the surface underlain by high salinity water derived from offshore. Between station PL-4 and PL-24, the longitudinal salinity variation in the near-bottom waters was approximately 2‰. Positions of the outer, middle and inner fronts are roughly at stations PL-3, PL-9 and PL-20, respectively.

The vertical distribution of specific gravity (σ_t) is shown in Figure 12b. The location of the inner front, the boundary between the well-mixed coastal zone and the stratified inner shelf, is clearly indicated at PL-20.

The methane distribution along the PL is depicted in Figure 12c. A bottom source of methane is apparent near station PL-6 and a secondary maximum at station PL-14. Both features seem to correlate with isolated pools of cold water as shown in Figure 12d. Maximum near-bottom concentrations of methane are associated with water $\leq 4^\circ\text{C}$. Surface concentrations range from near 300 nL L offshore to approximately 500 nL L in the coastal zone.

The areal extent of the near-bottom methane plume in August, 1980 is shown in Figure 13. The highest concentration (2500 nL L⁻¹) was observed

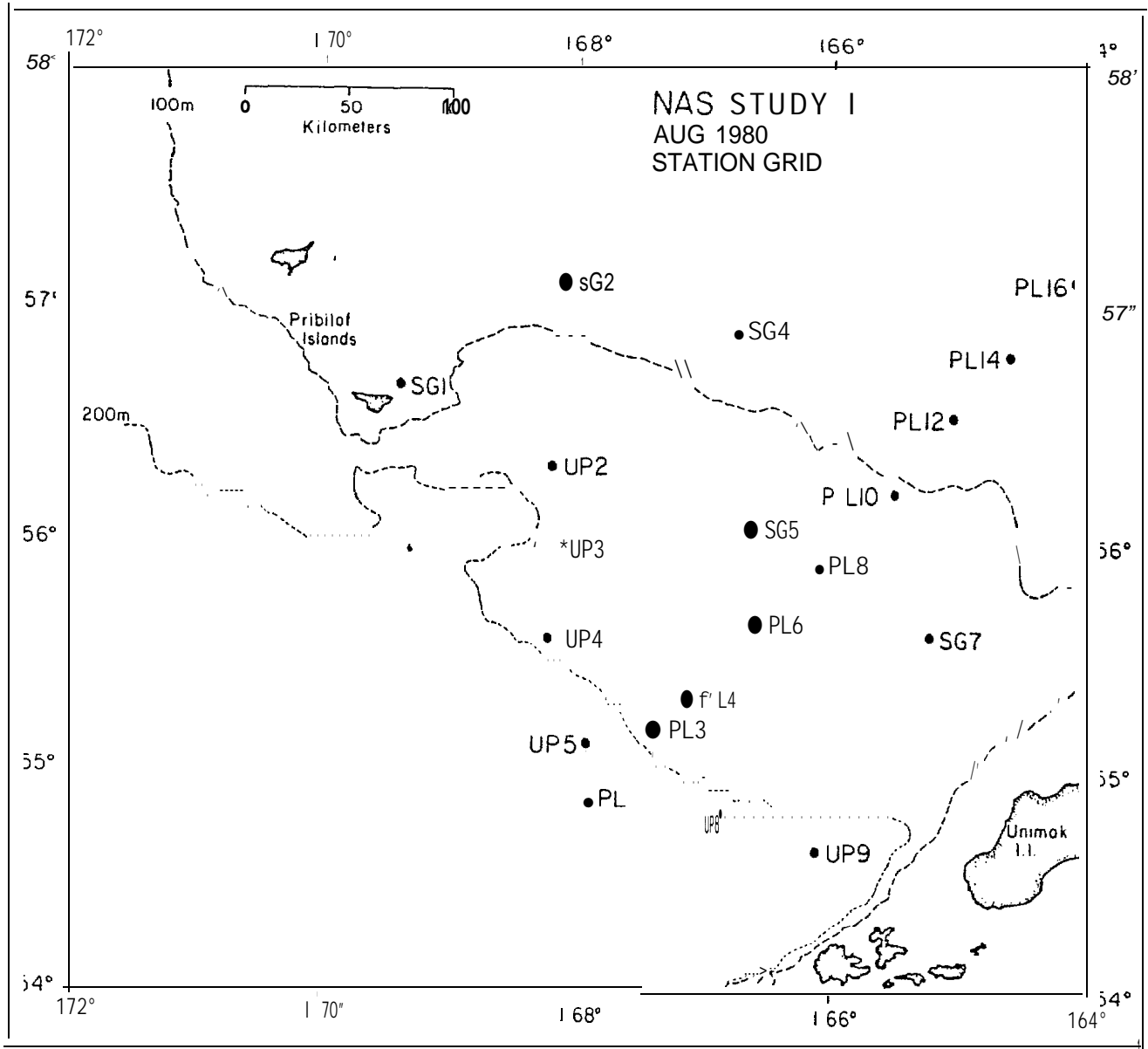


Figure 11. St. George Basin stations occupied in August, 1980.

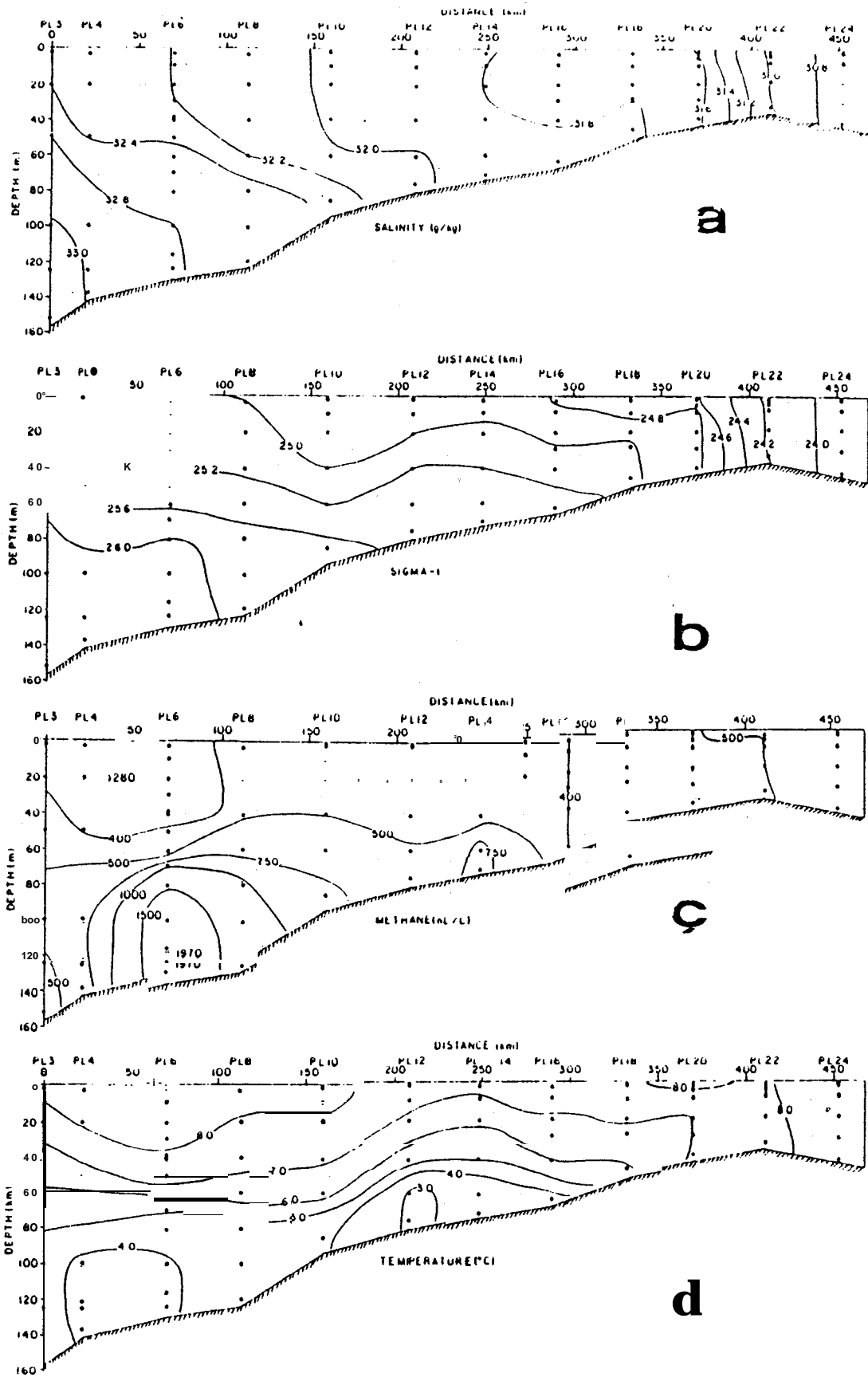


Figure 12. Vertical distribution of salinity (a), σ_t (b), methane (c) and temperature (d) along the PROBES Line in August, 1980. The middle front is located near PL 8-10.

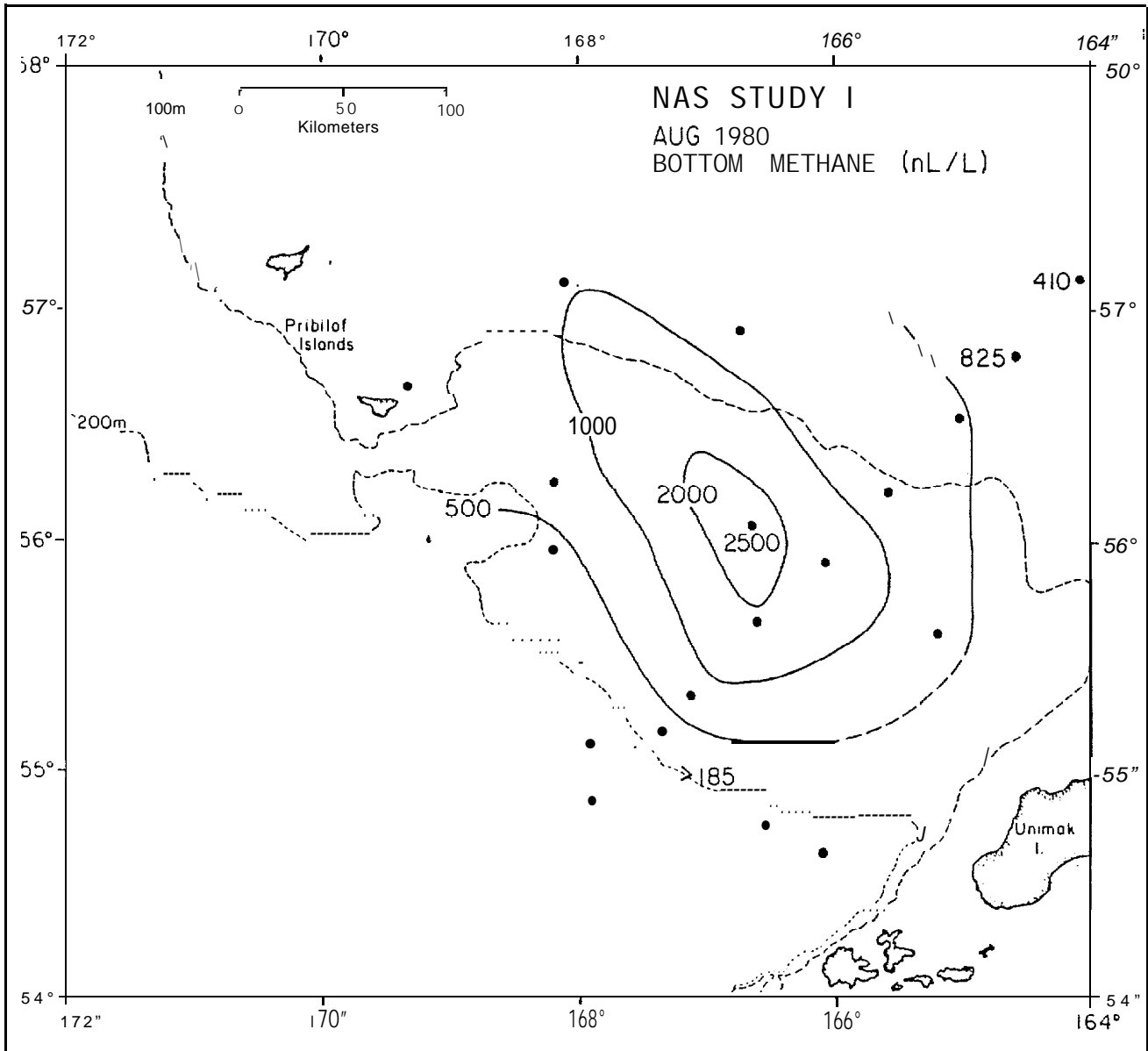


Figure 13. Near-bottom distribution (B-5 m) of methane (nL/L) in St. George Basin in August, 1980. Maximum concentrations were found near stations PL-6 and SG-5.

at SG-5, near PL-6. The plume trajectory shows a northwest-southeast orientation, which may be the result of anisotropic mixing or an elongated methane source. Although it is difficult to be precise, the plume structure appears to originate from a point source in the seafloor. If it is a gas seep, the methane appears to be of biological origin because of its compositional characteristics, that is, near absence of C_{2+} hydrocarbons.

The SBG station grid occupied in February, 1981 is shown in Figure 14. Because salinity, temperature and σ_t data were not available at the time of this writing, we are prepared to show only the vertical distribution of methane along the PL and the near-bottom concentration of methane is St. George Basin. The distribution of methane along the southwestern section of the PL is shown in Figure 15. Maximum near-bottom concentrations of methane were in excess of 500 nL L⁻¹ compared to background values near 200 nL L⁻¹.

The near-bottom methane plume, shown in Figure 16, is quite similar to the distribution observed in August, 1980. Again it appears that methane arises from a point source near PL-6 and disperses along an axis parallel to the isobaths. Maximum concentrations of methane observed were approximately 1500 nL L⁻¹, or approximately 1/2 the value observed in August. Without knowing specifically the nature of the methane source (i.e., biogenic or thermogenic), it is reasonable to assume a temporal variability in source strength. However, erosion of the pycnocline in February relative to August would also result in reduced methane concentrations because of an increased vertical flux that would be accommodated by a concomitant increase in the air-sea exchange flux.

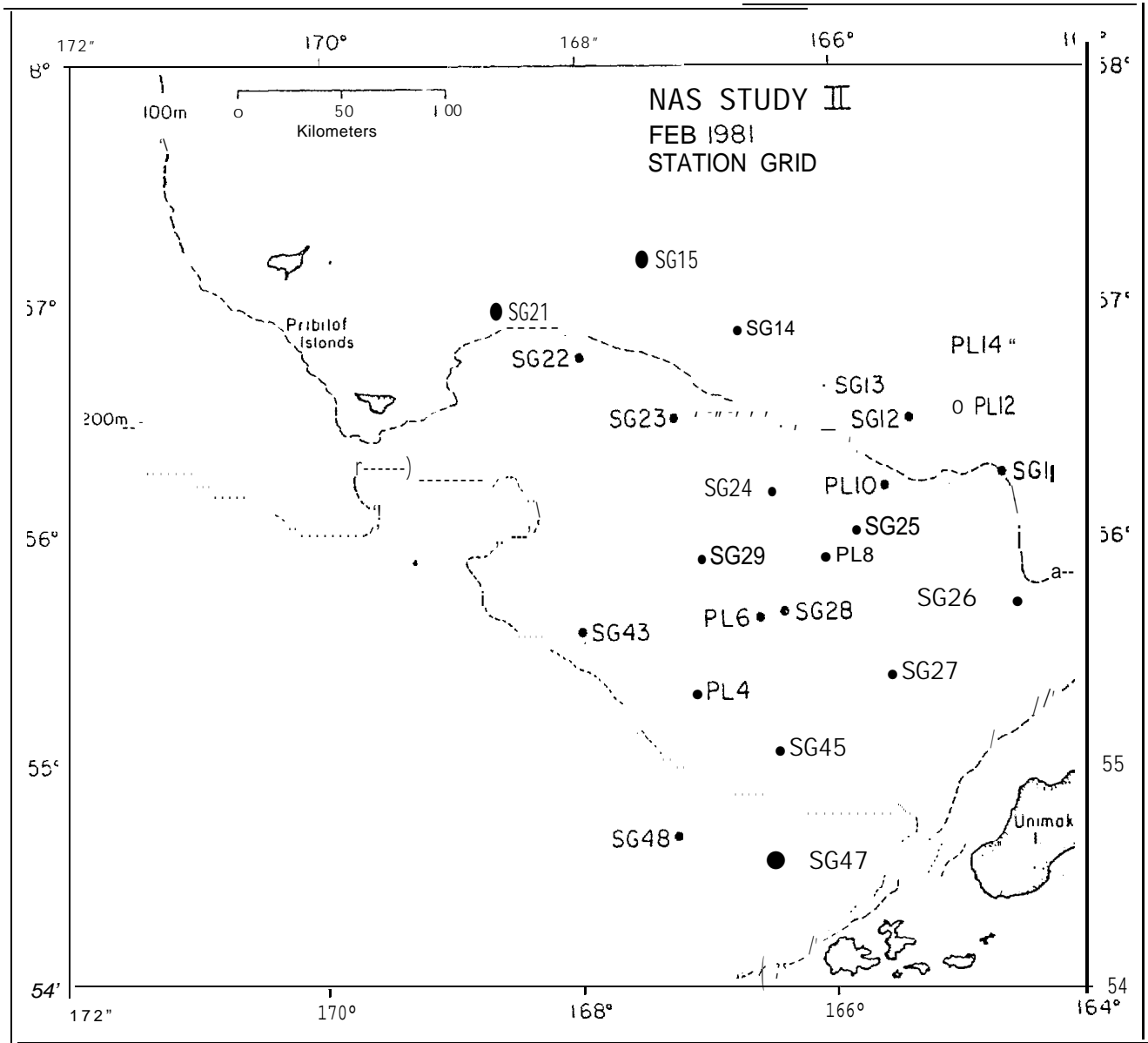


Figure 14. St. George Basin stations occupied in February, 1981.

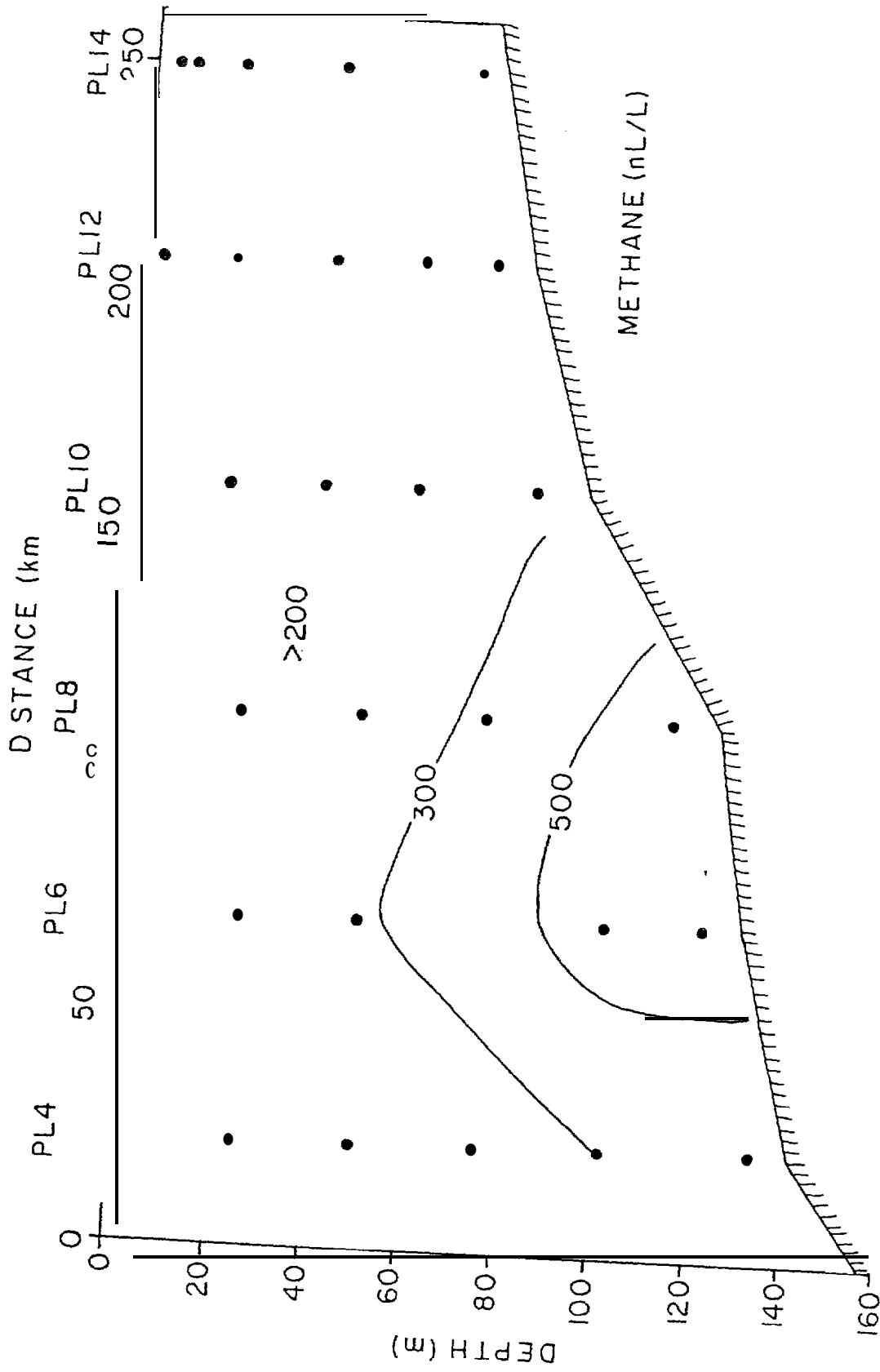


Figure 15. Vertical distribution of methane along a portion of the PROBES Line in February, 1981.

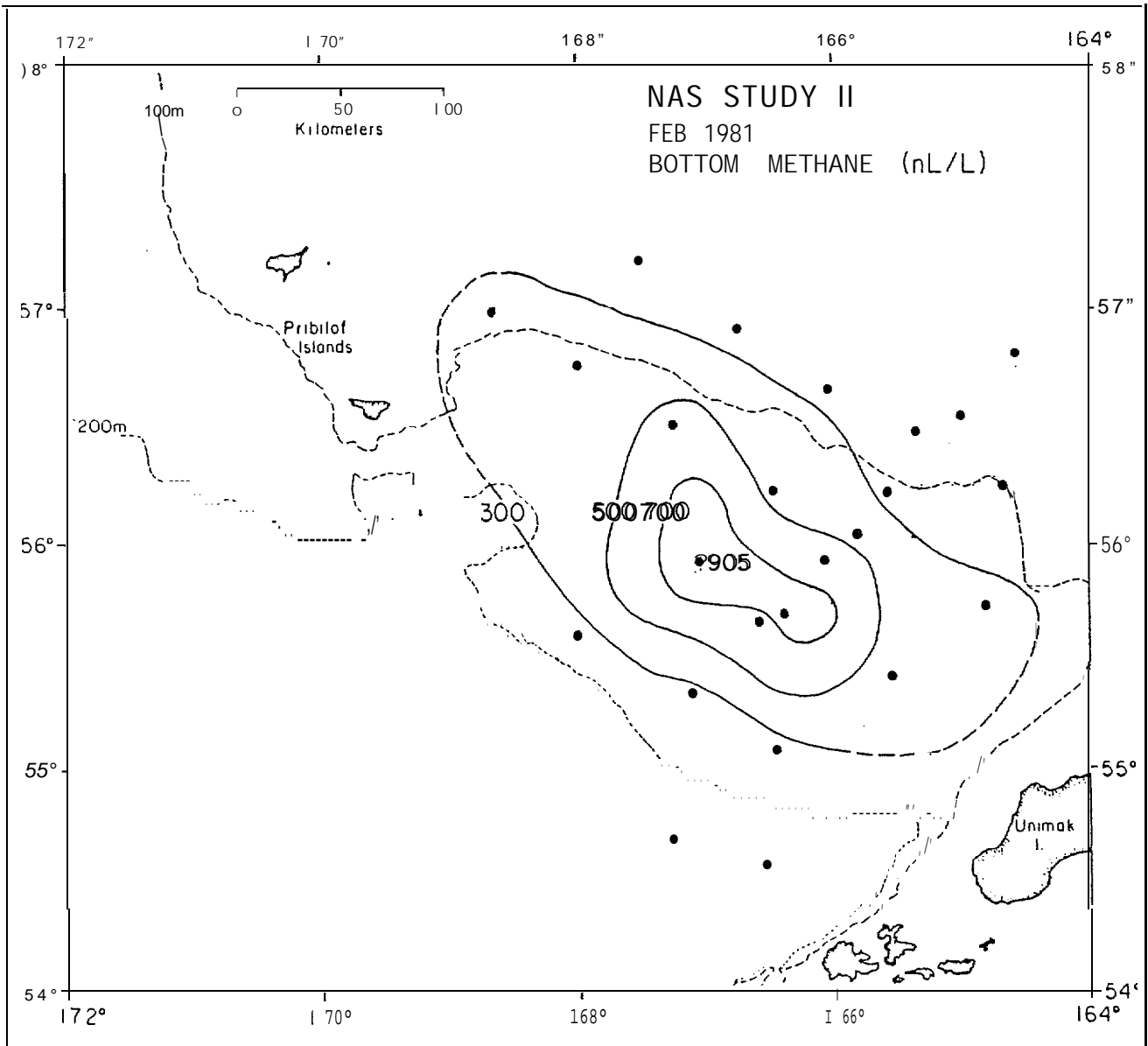


Figure 16. Near-bottom distribution (B-5 m) of methane (nL/L) in St. George Basin in February, 1981. Maximum concentration was observed at station SG-28; which is south of PL-6.

6. DISCUSSION

6.1 Plume Model

The distribution of dissolved methane along the NAS and in SBG is used to define limits on the horizontal and vertical eddy diffusivities and to compare mean flow velocities with those predicted from moored current meters. Because the program is still underway, only the August cruise data from the NAS will be considered in this report, but inferences about circulation processes in SBG will be made on the basis of preliminary data at hand.

To extract the salient spatial features of dissolved methane along the NAS, we adopted a stationary two-dimensional plume model described by Csanady (1973). The model has been used to predict the dispersion characteristics of wastewater injected from a pipe into a coastal zone. The model assumes stationary conditions, balances lateral diffusion against horizontal advection and includes a first order loss term. For stationary conditions:

$$\frac{\partial}{\partial y} \left[K_y \frac{\partial c}{\partial y} \right] - u \frac{\partial c}{\partial x} - kc = 0. \quad (1)$$

The solution to equation (1) for line source of length b is:

$$c = (c_0/2) \exp(-kx/u) [\operatorname{erf}(y^*_1) + \operatorname{erf}(y^*_2)], \quad (2)$$

where $y^*_1 = \frac{b/2 + y}{0.1039(x/u)^{1.17}}$

$$y^*_2 = \frac{b/2 - y}{0.1039(x/u)^{1.17}}$$

x = longshore direction

y = cross-shelf direction

u = longshore mean velocity

k = first order rate constant

c_0 = concentration of methane at the source

In the above model, we ignore diffusion in the x-direction and scale the horizontal diffusivity (K_h) in the y-direction according to the Lagrangian time scale. For simplicity, we assume that mixing is isotropic in the x- and y-directions. However, Okubo (1971) has shown that dispersion is enhanced in the direction of mean flow relative to dispersion across streamlines. The magnitude of the difference is approximately a factor of three for those coastal situations that have been studied. Furthermore, tidal currents are rectilinear along the shelf which likely results in an enhanced mixing alongshore. In the presence of a mean flow \bar{u} , it can be shown that:

$$\sigma_{rc}^2 = 2\sigma_x\sigma_y \quad (3a)$$

where σ_{rc} is the mean square radius of diffusing substance, σ_x and σ_y are the respective standard deviations of the plume in the x- and y-directions (Okubo, 1971). If we assume uniform horizontal mixing ($\sigma_{rc}^2 = 2\sigma_y^2$) the apparent diffusivity defined by Okubo is:

$$K_h = \sigma_y^2/4t \quad (3b)$$

or

$$K_h = \sigma_h^2/2t \quad (3c)$$

where $\sigma_h^2 = 2\sigma_y^2$ and t is the diffusion time. The characteristic time (or length) scale can be computed from $t = x/\bar{u}$. Substituting into (3c), we obtain:

$$K_h = \sigma_h^2 \bar{u}/2x \quad (3d)$$

Based on numerous dye patch studies, Okubo (1971) given estimates of K_h in terms of the characteristic length scale ℓ . He found that the 4/3 law tended to overestimate the magnitude of K_h and presented a log regression diagram that shows:

$$K_h \propto \ell^{1.1} \quad (3e)$$

or that

$$\sigma_{rc}^2 = 0.0108 t^{2.34} \quad (3f)$$

In equation (2), the horizontal eddy diffusivity is formulated in terms of the variance of the plume in the y-direction $Sy(\sqrt{2} \sigma_y)$. After substitution of $t = x/\bar{u}$ into (3f) we find:

$$\sqrt{2} s_y = 0.1039 t^{1.17} \quad (3g)$$

Based on the diffusion diagram given by Okubo (1971), we anticipate $10^5 \text{ cm}^2 \text{ s}^{-1} \leq K_h \leq 10^7 \text{ cm}^2 \text{ s}^{-1}$ for length scales between 10 and 100 km. If we assume that K_h is proportional to the tidal excursion, which is approximately 10 km, then $K_h \approx 10^5 \text{ cm}^2 \text{ s}^{-1}$. Because cross-shelf mixing is orthogonal to the isopycnal surfaces, the magnitude of the apparent horizontal diffusivity in the y-direction should be less.

Dissolved methane may be lost from the water column via air-sea exchange and biological oxidation. Since both processes can be formulated in terms of first order kinetics, they are included in the model as a single term:

$$k = k_{a/s} + k_{biol} \quad (a)$$

Computation of $k_{a/s}$ requires knowledge of sea-surface roughness (a function of wind speed), the molecular diffusion and Bunsen volatility coefficients of methane as a function of salinity and temperature. All of these parameters are known to within 30% (Broecker and Peng, 1974), thus $k_{a/s}$ can be estimated (see Cline, 1981 for details on the calculation of $k_{a/s}$).

Biological oxidation rates of methane, not previously known for these waters, have been determined by RU# 595 headed by Dr. Griffiths. Water samples were inoculated with a known amount of $^{14}\text{CH}_4$ and incubated for 24 to 48 hours. The $^{14}\text{CO}_2$ given off after oxidation was counted and the rate constant computed. The kinetics generally obeyed a first order reaction when incubation time and substrate levels were varied.

By averaging all the biological oxidation rate determinations made at stations NA-20 through NA-46 (see Fig. 3), we compute a first order biological rate constant of $9.5 \pm 3.1 \times 10^{-8} \text{ s}^{-1}$. In contrast, the air-sea exchange term, $k_{a/s}$, was $3.7 \times 10^{-7} \text{ s}^{-1}$ assuming a mean wind speed at 10 m above the sea surface of 5.7 ms^{-1} and a mean mixed layer depth of 30 m (see Cline, 1981.). Thus the air-sea exchange term is approximately four times the biological consumption term. The combined rate constant, k , is $4.6 \times 10^{-7} \text{ s}^{-1}$.

The model is formulated in terms of a line source of length b . If the depth of the mixed layer (Δz) is known, then the mass transport of methane out of Port Moller is simply:

$$Q_{\text{CH}_4} = (b) \cdot (\Delta z) \cdot (\bar{u}) \cdot (C_0) \quad (5)$$

where the mass transport Q has dimensions MT^{-1} . Thus, the model is sensitive to the boundary conditions: b , source length; Δz , mixed layer depth; \bar{u} , mean alongshore velocity; and C_0 , initial concentration at the boundary. Time

series measurements at the mouth of Port Moller were used to estimate b (8 to 10 km) and C_0 (4000 nL L^{-1}). The mean mixed layer depth (Δz) between shore and 10 km off shore was determined to be 15 m. The mean alongshore velocity (\bar{u}) was set so as to match the plume characteristics. The model does not take into account a time dependency of the source which appears to be applicable in light of the wave nature of the methane distribution along the NAS.

A schematic representation of the NAS and the major transport terms used in the model is shown in Figure 17. Because the water depth increases systematically as one moves offshore, the methane distribution in the 15 m surface layer must be vertically averaged to provide a realistic representation of the actual distribution. Under actual conditions, it appears that turbulent mixing in the coastal zone ($z \leq 50 \text{ m}$) is sufficient to maintain vertical homogeneity in most water properties.

6.1.1 Model Scenarios

In this section we present three model scenarios which attempt to bracket the mean velocity field of the coastal zone. The three cases representing mean alongshore velocities of 5, 7.5 and 10 cm s^{-1} , are shown in Figures 18 a, b and c. We selected a 5% contour interval as the minimum detectable level based on a source strength of 4000 nL L^{-1} and two times the ambient noise level in the methane data of 100 nL L^{-1} .

At a mean velocity of 5 cm s^{-1} , the effects of lateral diffusion are rather obvious in which the maximum excursion offshore is about 15 km (y) from a source length of 8 km (Fig. 18a). Maximum offshore penetration occurs at about 60-70 km downstream (x). Increasing the mean velocity " causes the plume to elongate in the downstream direction, systematically

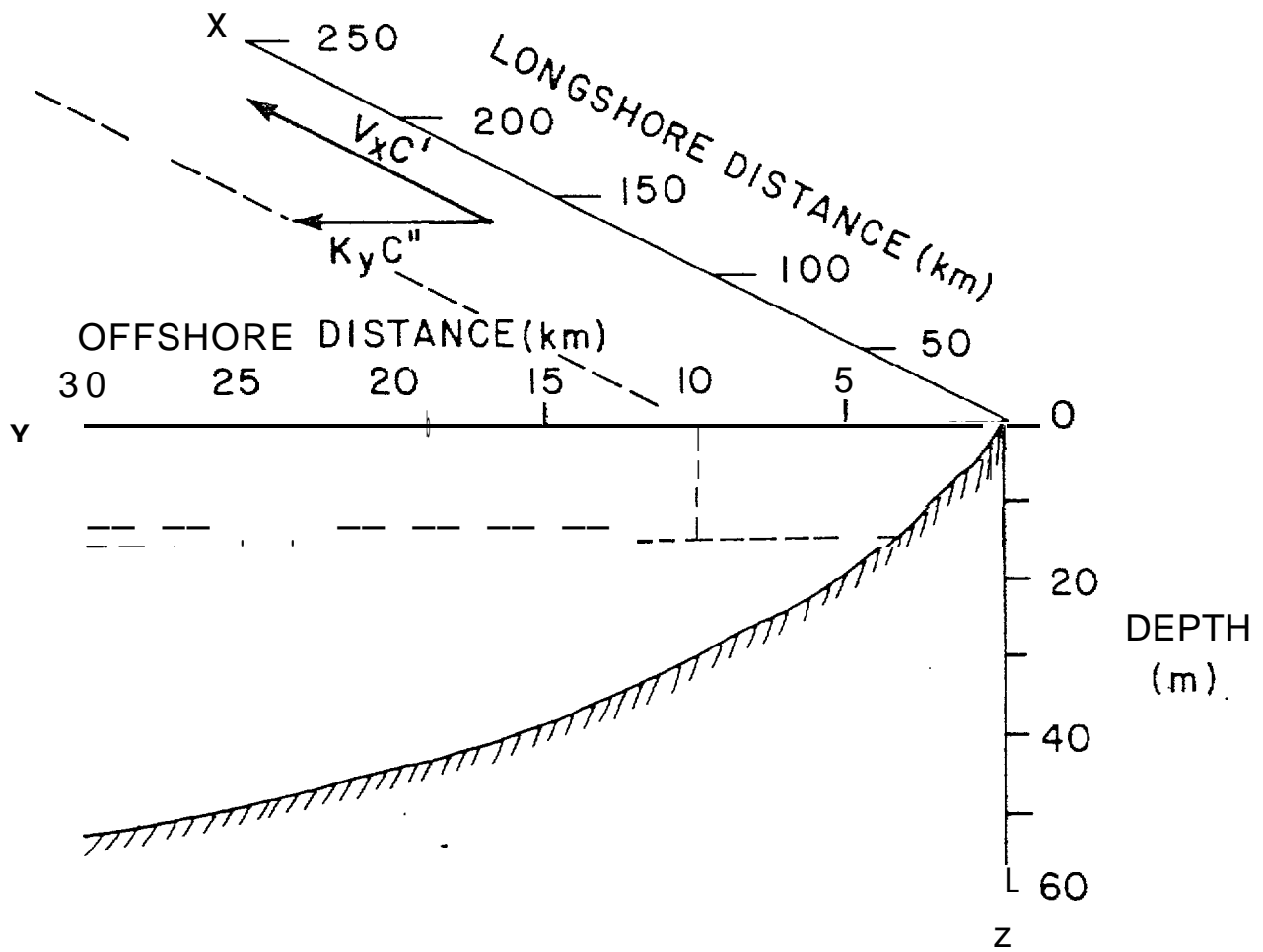


Figure 17. Model schematic of the NAS. The significant transport terms are horizontal diffusion, $K_y C''$, and horizontal advection, $V_x C'$. The well mixed coastal water is 10 km wide and 15 m deep.

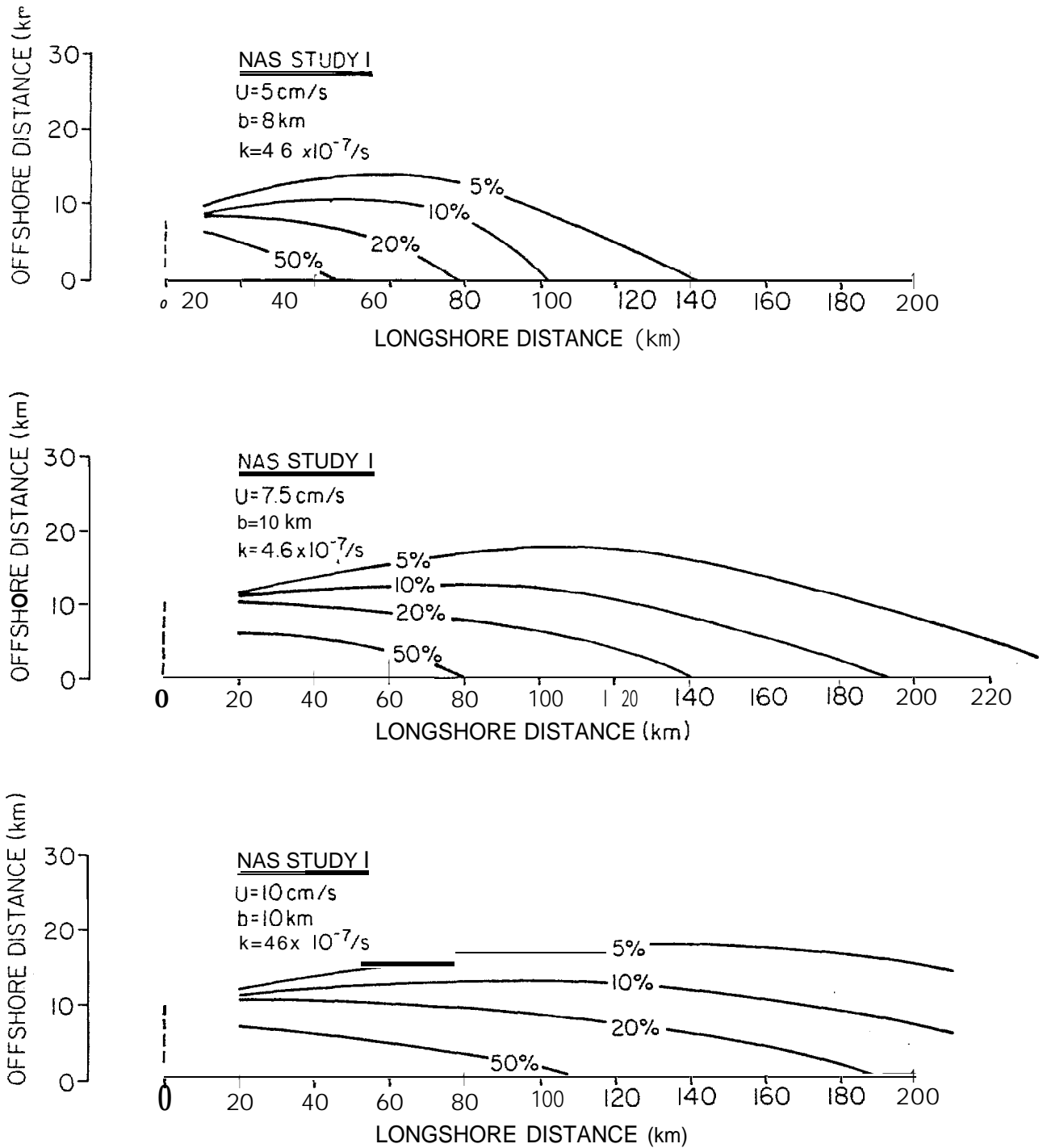


Figure 18. Relative concentrations of methane, depth integrated, predicted from equation (2), assuming various mean velocities of (a) 5 ems, (b) 7.5 cm s and (c) 10 cm s. Air-sea exchange of methane and biological oxidation are included in a single first order rate constant, $k = 4.6 \times 10^{-7} \text{ s}^{-1}$. Source strength is set at 8-10 km.

shifting the position of maximum excursion downstream (Figs. 18 b and c). As the velocity increases, lateral diffusivity becomes less important and the plume is contained largely within 10 km of shore or within the source distance b .

6.1.2 Model Fit

The depth averaged methane concentrations are shown in normalized form in Figure 19. Depth averaged concentrations at all stations outside the plume averaged $430 \pm 40 \text{ nL L}^{-1}$ (1σ). For comparison, we show the 10% isopleth for the model scenario of $\bar{u} = 7.5 \text{ cm s}^{-1}$ (Fig. 18b). Clearly, transport processes in the coastal zone are not as simple as the assumed model. The most serious discrepancy occurs at the input boundary, where episodically methane penetrates more than 10 km offshore. This results in a longitudinal wave structure. It is not clear whether accelerated pumping of the estuary occurs at selected tidal stages (e.g., perigean) or that some complex circulation occurs along the front between the well-mixed coastal zone and the more stratified water offshore.

Assuming a mean velocity of 7.5 cm s^{-1} , the node appearing at 105 km downstream is about 16 d downstream from the entrance to Port Moller. The daily tidal range and maximum tidal currents calculated for Entrance Point are plotted in Figure 20. The perigean tides, which occur every 28 d, appear to correlate well with the observed wave feature shown in Figure 19. Measurements, made along section VI (Fig. 19) on August 22, 1980, correlate well with the maximum perigean tidal excursion that occurred August 6-8, or about 16 d earlier. Because the station grid (Fig. 19) was occupied from east to west, section III (Port Moller) was occupied on August 24, 1980, about the time that a new perigean cycle was commencing (see Fig. 20). At about the same time however, the longshore winds were blowing toward the west (ap-

NAS STUDY I

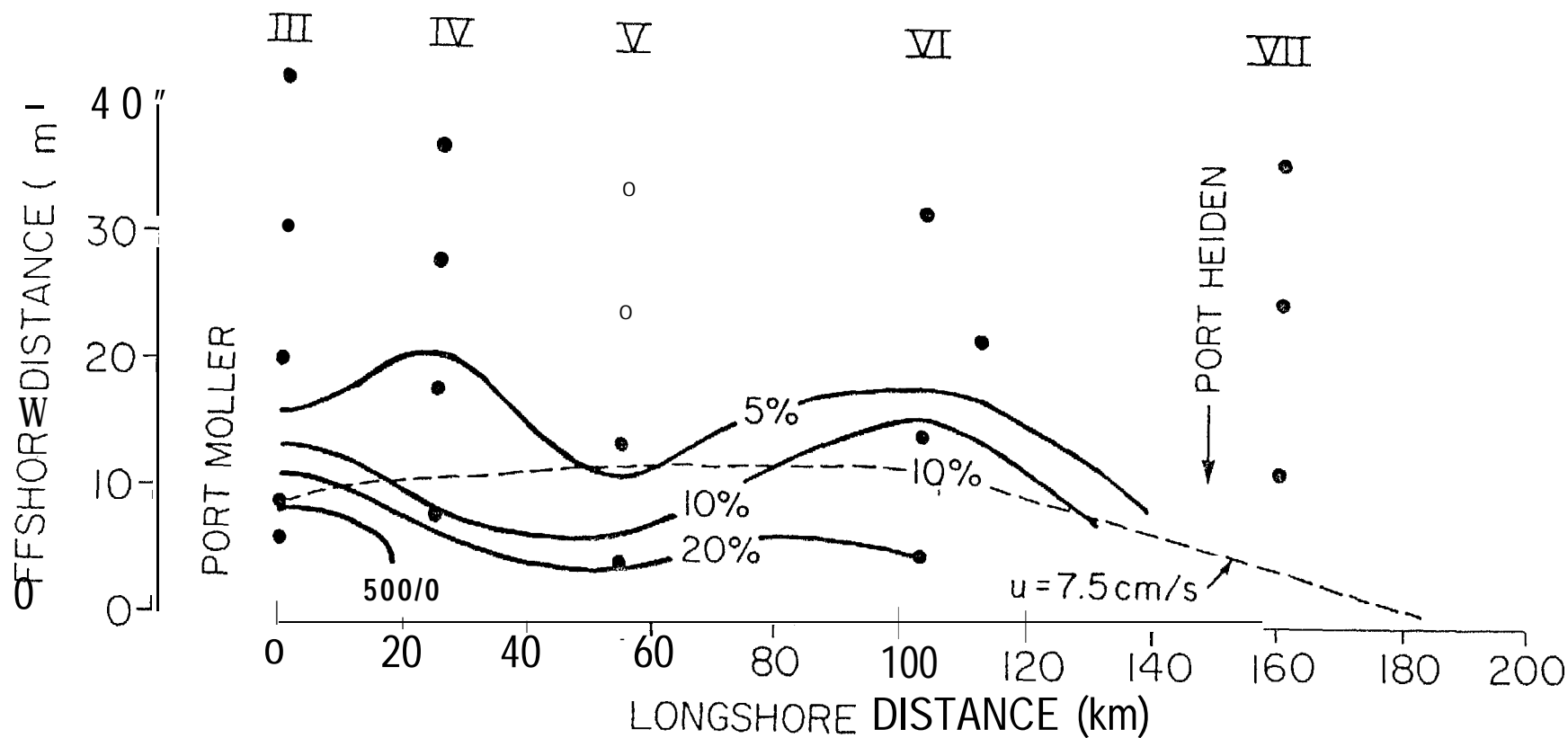


Figure 19. A comparison of a observed methane distribution (solid lines) with the 7.5 cm s model scenario. Pulsing of the estuary leads to a strong time dependent source, which is not accommodated by the stationary model.

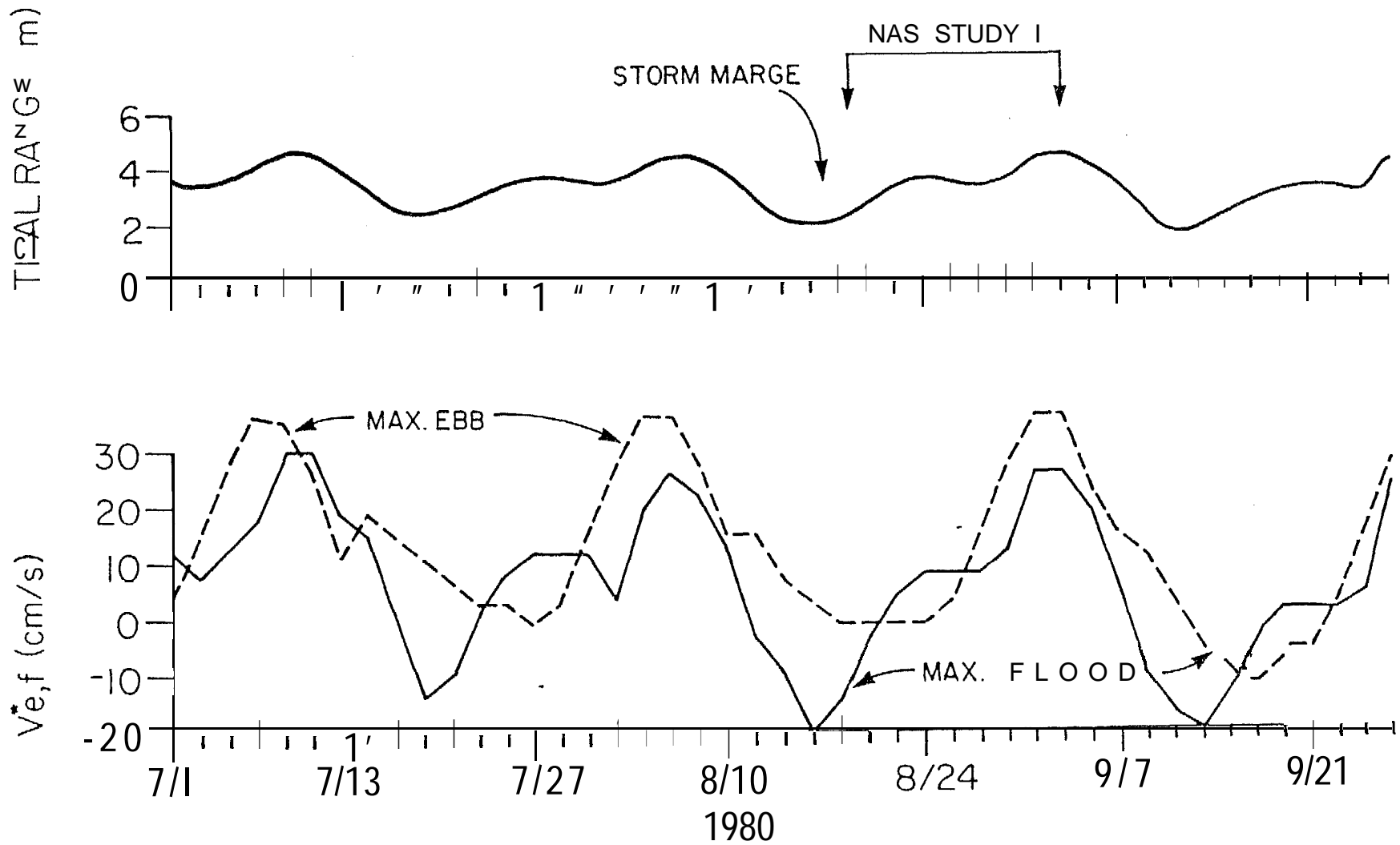


Figure 20. Tidal range and maximum ebb and flood tidal velocities at Entrance Point, Port Moller. The data presumably reflect conditions at mid-channel. Data are from the NOAA tide tables covering the observational period.

proximately 6 m S-l), inducing a strong Ekman surface flux offshore (Pearson et al., 1981). Assuming a mean offshore surface velocity of 4 cm s^{-1} for the period August 21-24, dissolved methane would penetrate about 10 km offshore. This is roughly the distance shown in Figure 19, but undoubtedly both tides and wind-induced Ekman transport worked in concert to produce the observed distribution.

The reason why estuarine tidal pumping is an attractive mechanism for an efflux of methane from Port Møller is related to the probable methane source. It is now suspected that the major source of methane is in Herendeen Bay, a small isolated deep basin (approximately 100 m) with a shallow sill (approximately 22 m). Both the concentration of methane and the methane production rate (Griffiths, 1981) were highly elevated in this fjord-like bay in February, 1981. If flushing of this bay occurs primarily by tidal forces, we expect it to occur most likely during spring and perigean tidal cycles. During quiescent periods, the waters below sill depth would be stabilized, allowing methane concentrations to increase significantly. Obviously flushing would be enhanced by the presence of more dense water offshore, which presumably has a seasonal signature.

The distribution of methane as shown in Figures 4 and 19 suggests a mean drift east along the coast at a velocity of 5-10 cm S-l. The characteristic time scale for these velocities is 17-35 d, thus our model predictions are not sensitive to tidal and subtidal events (2-10 d). Wind and current measurements made between August 20 and September 2 (13 d) suggest little mean current either east or west along the coast (Pearson et al., 1981). Surface mean currents are related to wind trajectories lasting for 2-4 d, causing directional Ekman transport along the coast (Pearson et al., 1981). The reasons for the disparity between measured mean current velocities and

the observed trajectory of the methane plume is not known, but several explanations are offered for discussion.

The current meter record is for 13 d and may not allow a statistical comparison to be made. There also may be difficulties associated with the extraction of subtidal frequencies ($0.001\text{-}0.002\text{ hr}^{-1}$) when the energy spectrum is so heavily dominated by tides. It is also possible that non-linear tidal effects are present that lead to a net transport eastward along the NAS coastal zone. If non-linear tidal effects are not important, then tidally-induced diffusion would not result in the observed distribution, since we expect tidal energy to be isotropic in the x-direction.

While this dilemma has not been solved, it is hoped that these results might generate additional thought concerning transport mechanisms along the near shore areas of the NAS. The impact of spilled oil in this region, particularly on the beach and into the intertidal zone, depends critically on flow trajectories over temporal scales of a few days to a few months. Methane distributions are shown to be useful over time scales of 10-30 d.

6.2 St. George Basin

Seasonal observations conducted during the past five years have shown the existence of a localized bottom source of methane in SGB (see Figs. 13 and 16). The location is centered about $55^{\circ}40'N$ and $167^{\circ}00'W$. Unfortunately, the spatial station resolution during both the August and February cruises was too coarse to clearly identify the nature of the source. Horizontal diffusion coupled with episodic cross-shelf currents tend to confuse the exact nature of the source. One also could postulate a line or rectangular source which would not be inconsistent with the observed distributions.

6.2.1 Vertical Methane Distribution

Before describing a few of the prominent features of the methane distribution in SBG, we first address the vertical structure observed in August. At station PL-6 (see Fig. 11) located near the center of the middle shelf, the vertical density distribution (Fig. 21) reflects processes of salt fingering and double diffusion (Coachman and Charnell, 1977). Station PL-6 was occupied twice during the cruise, the time interval between visits was about 5 d. The points of interest are the well-mixed surface layer ($\Delta z_s \simeq 30$ m) and bottom boundary layer ($\Delta z_b \simeq 30$ m). Between these layers, the density gradient is sharp, but not uniform. Because of the degree of stratification present, a barrier to vertical transport of materials from the bottom boundary is expected. To quantify the magnitude of the relevant vertical transport parameter, K_v , within the pycnocline, we adopted a one-dimensional flux model describing the vertical distribution of dissolved methane. The vertical distribution of methane at station PL-6 for the two observational periods is shown in Figure 22. Measurements taken on September 3 were used in the model because they were more detailed.

The one-dimensional flux model assumes that the curvature in the methane profile is derived from a variable vertical eddy coefficient and not the result of in situ consumption. This assumption may or may not be valid, but as we show below, it places an upper limit on the magnitude of K_v . The essence of the model is that the methane is produced in the bottom boundary layer (or the underlying sediments). Most of the methane produced is removed (by horizontal diffusion and advection), however some fraction fluxes vertically through the pycnocline and is removed by air-sea exchange (stationary conditions). In the absence of horizontal or biological processes adding or removing methane, the model for the pycnocline is:

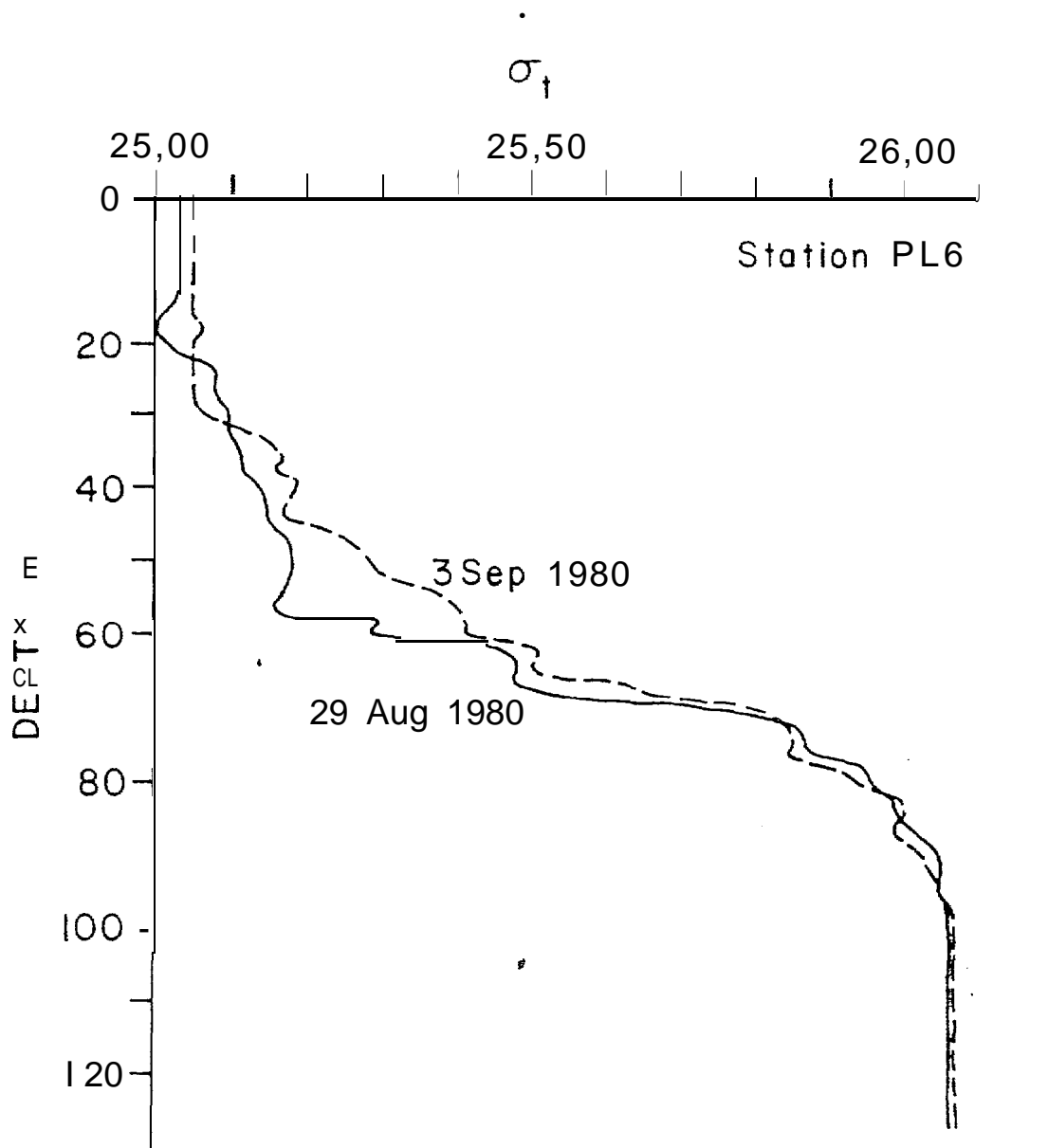


Figure 21, Vertical density distribution at PL-6 on August 29, 1980 and September 3, 1980. Note the effects of salt fingering and double-diffusion.

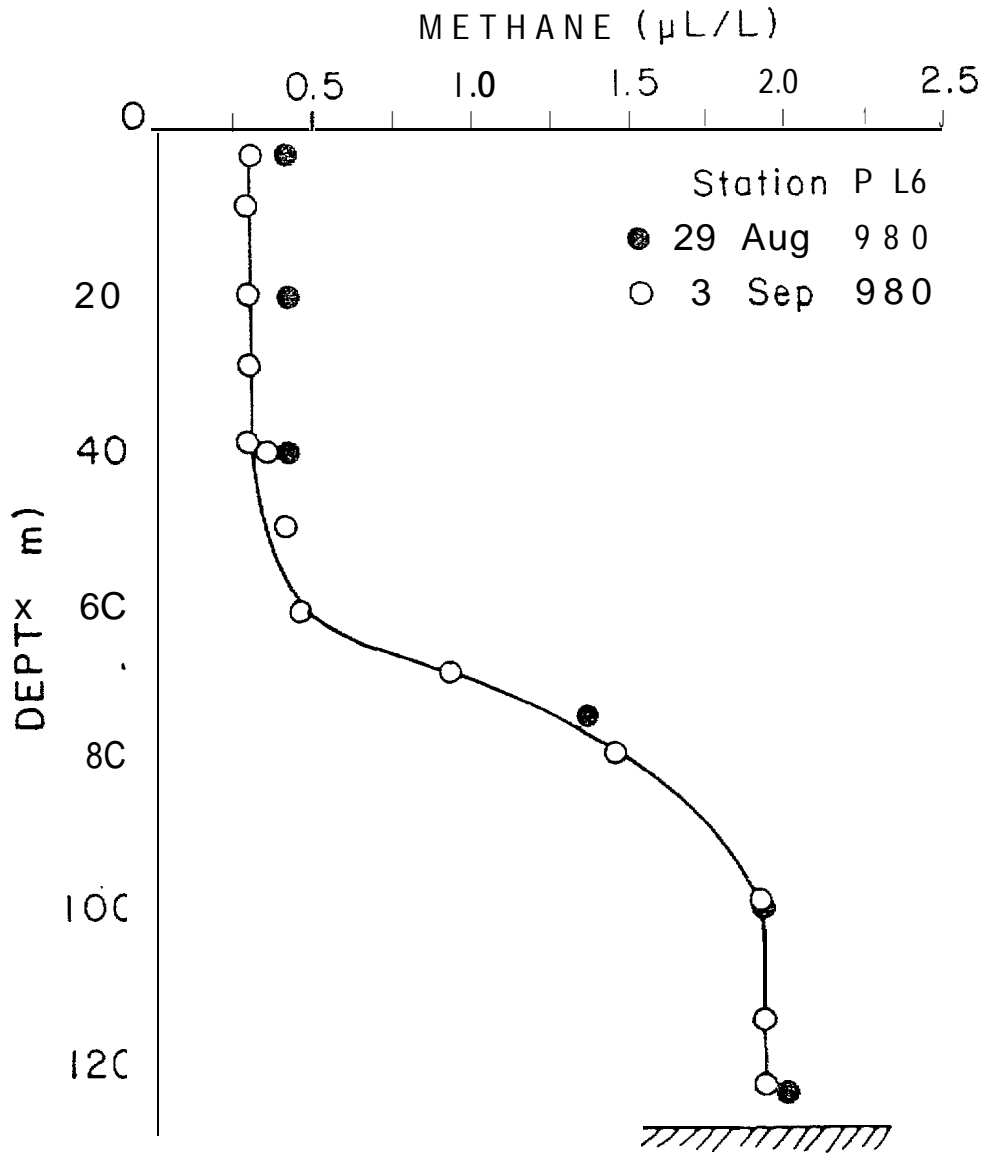


Figure 22. Vertical distribution of dissolved methane at PL-6 on August 29, 1980 and September 3, 1980.

$$K_v \frac{dC}{dz} = \text{constant} \quad (6)$$

where K_v is the depth dependent vertical eddy diffusivity. Since the flux across any horizontal plane is a constant, that constant must be equal to the air-sea exchange flux:

$$F_{a/s} = \frac{D}{\Delta h} (C - C') \quad (7)$$

where D is the molecular diffusivity of dissolved methane, Δh is the thickness of the stagnant film boundary layer and C' is the equilibrium solubility of methane at the surface. For the surface conditions during the cruise, $F_{a/s} = 1.9 \times 10^{-4} \text{ nL cm}^{-2} \text{ s}^{-1}$. The uncertainty in this value is no more than a factor of 2. To derive the functional dependence of K_v , the methane profile was smoothed by hand and a cubic spline function was fit to the curve. This function was then differentiated and used to calculate the gradient in equation (6).

Rather than present the estimated values of K_v as a function of depth, we plot them against the Brunt-Väisälä frequency, a measure of stability (Welander, 1967). The relationship is shown in Figure 23. The data separate into two distinct groups, both of which show a reciprocal $1/2$ power relationship. Based on the theoretical arguments presented by Welander (1967), this correlation implies turbulence induced by shear, which intuitively is not surprising. The dashed lines show the reciprocal $1/2$ power relationship without data regression.

In the upper portion of the pycnocline ($24 \text{ m} < z < 50 \text{ m}$), K_v varies from about $20\text{-}50 \text{ cm}^2 \text{ s}^{-1}$. Because of the sluggishness of air-sea exchange, the methane flux model is not useful when vertical eddy diffusivities exceed

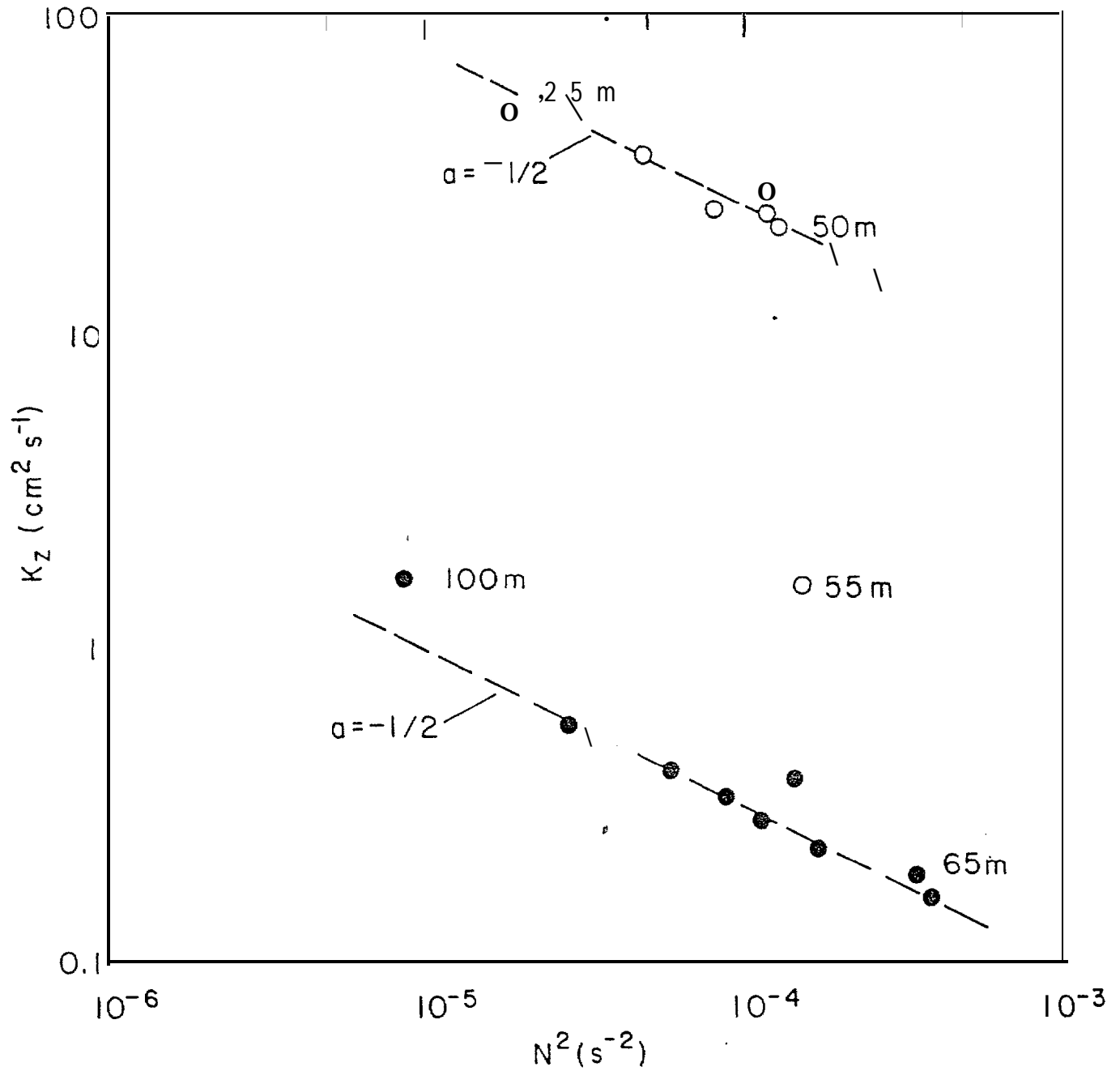


Figure 23. Estimated apparent vertical eddy diffusivity or a function of the buoyancy gradient. The Brunt-Vaaisela frequency was determined from the density distribution; K_z from the observed methane profile. The reciprocal square-root relationship suggests shear-induced turbulence.

$50 \text{ cm}^2 \text{ s}^{-1}$. In the lower portion of the pycnocline, K_v varies from 0.15 to $1 \text{ cm}^2 \text{ s}^{-1}$. Between these two regions, eddy diffusivity decreases rapidly and separates the water column into two distinct energy regimes. Near the surface, K_v is much larger because horizontal shear is the dominant mechanism by which energy is released to turbulent mixing. The lower region of the pycnocline is the principal concern in terms of bottom-released material. Between 65-95 m, the average K_v is about $0.3 \text{ cm}^2 \text{ s}^{-1}$ and will provide significant resistance to the vertical transport of dissolved and emulsified oil.

Returning to the model assumptions, boundary conditions could have been satisfied with either a bottom or surface flux. Microbial production rates in the sediments near PL-6 measured in August (Griffiths, 1981) gave an estimated surface flux of $5.8 \times 10^{-4} \text{ nL cm}^{-2} \text{ S}^{-1}$ or about a factor of 3 greater than the computed air-sea flux. As already noted, a large fraction of the methane is removed by lateral processes, hence the production rates quoted above are not unrealistic. If the methane is coming from a point source in the sea floor and is of thermogenic or paleomicrobial origin, then the measured production rates are not relevant to an understanding of the plume dynamics. Because of these uncertainties, we adopted an air-sea exchange flux as the boundary condition.

It has been assumed that there is no in situ methane consumption or production. If we now assume that biological oxidation occurs in the lower portion of the pycnocline ($65 \text{ m} < z < 95 \text{ m}$), the resultant methane concentration profile would show an increased curvature. Therefore, K_v would have to be even smaller than the estimated 0.15 to $1 \text{ cm}^2 \text{ s}^{-1}$. Thus, the model predicts a maximum value of K_v . This can be seen in the following model analogy. Assume that methane is produced in a lower boundary layer and con-

sumed according to first order kinetics (Griffiths, 1981) in the pycnocline. Further assume that K_v is depth dependent as before. The conservation of mass in the vertical is (steady state):

$$\frac{\partial}{\partial z} [K_v \frac{\partial C}{\partial z}] - kC = 0 \quad (8)$$

Performing the differentiation, we obtain after rearrangement:

$$\frac{\partial C}{\partial z} = \frac{kC - K_v (\partial^2 C / \partial z^2)}{\partial K_v / \partial z} \quad (9)$$

Considering the lower boundary region we have $\partial K_v / \partial z > 0$; $K_v > 0$ and $\partial^2 C / \partial z^2 < 0$, thus the gradient becomes:

$$\partial C / \partial z = (kC + |K_v (\partial^2 C / \partial z^2)|) / \partial K_v / \partial z. \quad (10)$$

Therefore, the methane gradient is increased by biological consumption in the lower boundary layer ($\partial^2 C / \partial z^2 < 0$) and our previous flux model ($k = 0$) must overestimate the magnitude of K_v .

6.2.2 Near-Bottom Methane Plume

We earlier showed the distribution of dissolved methane in the near-bottom waters of SGB (Fig. 13). Because the lower 30 m or so of the water column is well-mixed, the area] distribution shown in Figure 13 represents rather well the depth integrated distribution. Assuming that most of the methane arises from a single source (near SG-5 and PL-6), the distribution might be analyzed in terms of a lateral diffusive model or a longitudinal advection-lateral dif-

fusion model. Mean currents in the near-bottom waters more toward the northwest at $2\text{-}5\text{ cm s}^{-1}$ (Kinder and Schumacher, 1981a). This mean current trajectory along shelf undoubtedly influences the observed orientation of the methane plume. We are not prepared at this time to analyze the methane plume in terms of a diffusion model with variable eddy diffusivities, but rather will use the diffusion-advection model already described for the NAS.

The model shown in equation (1), is modified slightly. Namely, the air-sea exchange flux is ignored since it is the lower boundary layer that is being analyzed. The source is estimated to be 30 km in length (cross-shelf) from Figure 13. Vertical diffusion is ignored and the mean velocity field is assumed to be in the range of $2.5\text{-}5\text{ cm s}^{-1}$, based on current meter measurements. The results for the 2.5 cm s^{-1} case is shown in Figure 24a (dashed lines) and compared to the actual normalized distribution. A visual fit of the observed depth integrated data to a velocity field of 5 cm s^{-1} is much better, as shown in Figure 24b. Thus, the plume morphology suggests a mean velocity to the northwest of 5 cm s^{-1} in good agreement with the accepted current velocities. In all likelihood, however, anisotropic lateral mixing would give a similar result.

If we accept the premise that methane arises from a localized source ($b = 30\text{ km}$), and the mean velocity field is near 5 cm s^{-1} , then the plume extension to the southeast is the result of complex mixing patterns not formally included in the model. Anisotropic lateral mixing ($K_y \neq K_x$), episodic reversals in mean flow and cross-shelf advection are all realistic options which, if included in the model, would probably give a realistic representation of the near-bottom methane distribution.

These results suggest that dissolved or emulsified petroleum compounds introduced into the near-bottom waters of SGB will move rectilinearly along

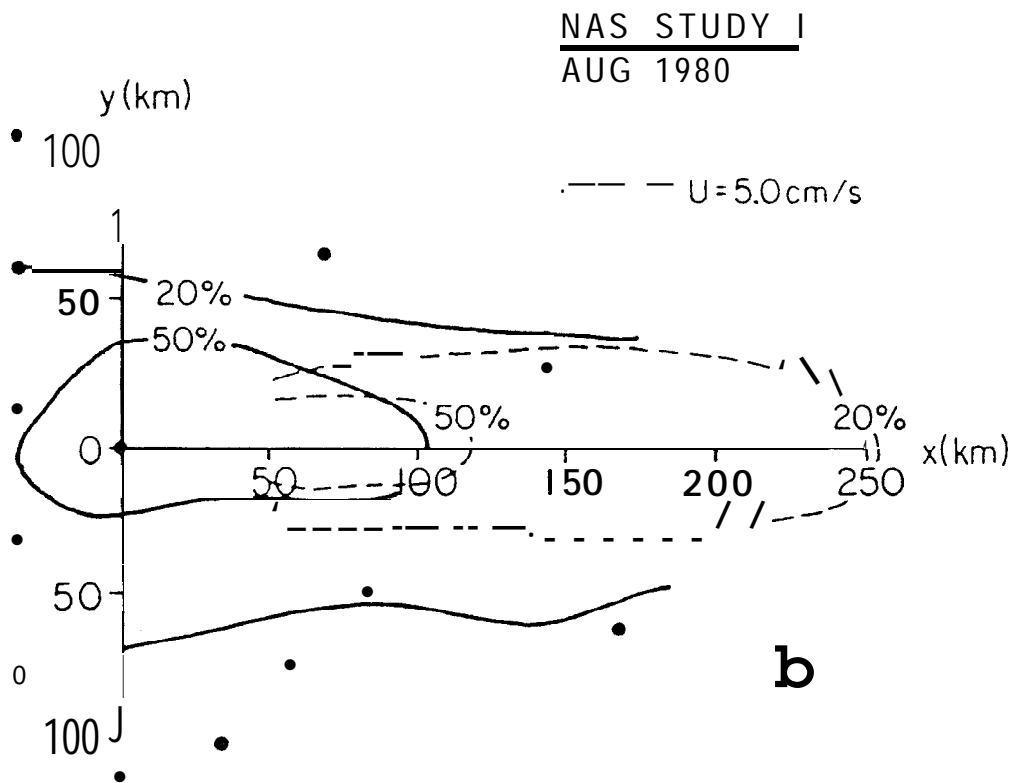
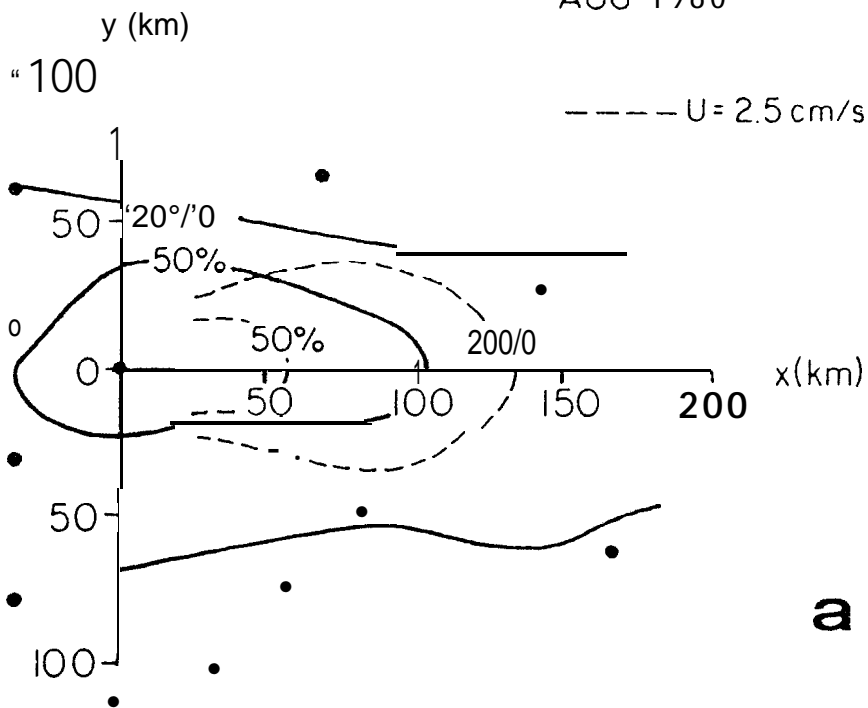


Figure 24. A model fit to the depth integrated methane profile in the lower boundary layer ($\Delta z \approx 30$ m). The two case studies are (a) $\bar{u} = 2.5 \text{ cm s}^{-1}$ and (b) $\bar{u} = 5.0 \text{ cm s}^{-1}$. The length of the source was assumed to be 30 km. The biological oxidation rate constant for the destruction of methane was set equal to $3.0 \times 10^{-8} \text{ s}^{-1}$.

the axis of the basin. There appears to be little on- or off-shelf penetration of methane which suggests that the outer and middle fronts are effective in restricting cross-shelf transport. We suspect that methane is introduced from a localized source, and thus, will mimic dissolved fractions of petroleum introduced in a similar manner.

REFERENCES

- BROECKER W.S., and PENG T.H. (1974) Gas exchange rates between air and sea. *Tellus* 26, 789-802.
- CLINE J.D. (1981) Distribution of dissolved LMW hydrocarbons in Bristol Bay, Alaska: Implication for future gas and oil development. In *The Eastern Bering Sea Shelf: Oceanography and Resources*, (eds D.W. Hood and J.A. Calder) Vol. 1, pp 424-444, Dept. Commerce/NOAA/OMPA, 625 pp.
- COACHMAN L.K. and CHARNELL R.L. (1979) On lateral water mass interaction - A case study, Bristol Bay, Alaska. *J. Phys.Oceanogr.* 9, 278-297.
- CSANADY G.T. (1973) Turbulent diffusion in the environment. D. Reidel Publishing, Boston.
- DEPARTMENT OF COMMERCE (1981) Tidal current tables 1981. Pacific coast of North America and Asia. NOAA, *National Ocean Survey*, 260 pp.
- GRIFFITHS R.P. (1981) Microbial processes as related to transport in the North Aleutian Shelf and St. George Lease areas. Annual Rept., OCSEAP/OMPA, 56 pp.
- KATZ C.N. (1980) Processes affecting the distribution of low molecular weight aliphatic hydrocarbons in Cook Inlet, Alaska. Master's Thesis, Univ. Washington, 131 pp.
- KINDER T.H. and SCHUMACHER J.D. (1981a) Hydrographic structure over the continental shelf of the southeastern Bering Sea. In *The Eastern Bering Sea Shelf: Oceanography and Resources*, (eds D.W. Hood and J.A. Calder) Vol. 1, pp. 31-52, Dept. Commerce/NOAA/OMPA, 625 pp.

- OKUBO A. (1971) Oceanic diffusion diagrams. *Deep-Sea Res.* 18, 789-802.
- OVERLAND J.E. (1981) Marine climatology of the Bering Sea. In *The Eastern Bering Sea Shelf: Oceanography and Resources*, (eds D.W. Hood and J.A. Calder), Vol. 1, pp. 15-22, Dept. Commerce/NOAA/OMPA, 625 pp.
- PEARSON C.A., BAKER E. and SCHUMACHER J.D. (1980) Hydrographic, suspended particulate matter, wind and current observation during reestablishment of structural front: Bristol Bay. EOA (Abstract)
- SCHUMACHER J.D., KINDER T.H., PASHINSKI D.H. and CHARNELL R.L. (1979) A Structural front over the continental shelf of the eastern Bering Sea. *J. Phys. Oceanogr.* 9, 79-87.
- SWINNERTON J.W. and LINNENBOM V.J. (1967) Determination of the C₁ to C₄ hydrocarbons in seawater by gas chromatography. *J. Chromatogr. Sci.* 5, 570-3.
- WELANDER P. (1967) Theoretical forms for the vertical exchange coefficients' in a stratified fluid with application to lakes and seas. *Acta Geophysica* 1, 1-27.